

Disturbance Observer Based Bilateral Control  
Systems

by

Abdurrahman Eray Baran

Submitted to the Graduate School of Sabancı University  
in partial fulfillment of the requirements for the degree of  
Master of Science

Sabancı University

August, 2010

# Disturbance Observer Based Bilateral Control Systems

APPROVED BY:

Prof. Dr. Asif Şabanoviç  
(Thesis Advisor)

.....

Assoc. Prof. Dr. Kemalettin Erbatur

.....

Assoc. Prof. Dr. Erkay Savaş

.....

Assist. Prof. Dr. Ahmet Onat

.....

Assist. Prof. Dr. Kürşat Şendur

.....

DATE OF APPROVAL:

.....

© Abdurrahman Eray Baran 2010

All Rights Reserved

# Disturbance Observer Based Bilateral Control Systems

Abdurrahman Eray Baran

ME, Master's Thesis, 2010

Thesis Advisor: Prof. Asif Şabanović

Keywords: Bilateral Control, Teleoperation, Transparency, Functional Observer, Disturbance Observer, Communication Disturbance Observer, Grasping Control, Adaptive Control

## Abstract

Bilateral teleoperation is becoming one of the far reaching application areas of robotics science. Enabling a human operator the ability to reach and manipulate a remote location will be possible with the various applications of bilateral control. In that sense, ideal bilateral control allows extension of a person's sensing to a remote environment by a master slave structure. So, the coupled goals of bilateral control is to enforce the slave system track the motion generated on the master system and to reflect the forces from the slave system. This thesis investigates the current state of the art in bilateral teleoperation. For that purpose, design and analysis of bilateral control is made based on the use of disturbance observers. First, a known control structure is investigated in the context of acceleration control. Following this, a case study is made to show a different application of bilateral control, namely grasping force control. Performance improvement in bilateral control is also studied and correspondingly, a novel functional observer is proposed for better estimation of velocity, acceleration and disturbance. In the second half of the thesis, bilateral control with time delay is realized. Design is made via separating the position and force into two different loops. For position control under time delay, a previously proposed control scheme is used in which use of communication disturbance observer with convergence terms was discussed. Observation made about the divergence from the master reference under contact motion is analyzed and a model following control structure is proposed to eliminate the remaining disturbance from the slave plant. For force control under time delay, first the response of a local controller is analyzed. In order to improve the system transparency, a

new method is proposed in which environment stiffness was used for force control loop rather than the delayed slave force. In this structure, estimation of environment stiffness was made via an indirect adaptive control scheme. The analyzed structures were also tested experimentally under a master slave system consisting of 1 DOF linear motors. Experiments show the validity of the contributions made for bilateral control with and without time delay.

# Bozucu Etmen Denetleyicisi Tabanlı İki Yönlü Denetim Sistemleri

Abdurrahman Eray Baran

ME, Master Tezi, 2010

Tez Danışmanı: Prof. Dr. Asif Şabanoviç

Anahtar Kelimeler: İki yönlü denetim, Teleoperasyon, Şeffaflık, Fonksiyonel Gözlemci, Bozucu etken gözlemleyicisi, İletişim bozucu etken gözlemleyicisi, Tutma kuvveti denetleyicisi, Uyarlanabilir denetim

## Özet

İki yönlü hareket denetim sistemleri robotik biliminin uzun vade uygulamaları arasında yerini almaktadır. İki yönlü denetimin değişik uygulamaları, bir kimsenin uzak noktalara erişimini ve uzaktaki bir ortamda hareketini mümkün kılabilir. Bu bağlamda, ideal iki yönlü denetim insanlara uzaktaki bir ortamı hissetme yeteneğini bir köle efendi yapısı sayesinde olanaklı kılmaktadır. Buradan hareketle iki yönlü denetimin temel hedefleri köle sistemin efendi sisteme uygulanan hareketi birebir tekrarı ve efendi sistemin köle sistemde hissedilen kuvvetleri operatör kişiye yansıtabilmesi olarak ifade edilebilir. Bu tezde, iki yönlü denetimin detayları incelenmiştir. Bu amaçla, bozucu etken denetleyicileri kullanılarak iki yönlü denetleyici analizi ve tasarımı yapılmıştır. İlk olarak, bilinen bir yapı ivme denetimi konseptinde analiz edilmiş ve denenmiştir. Bunu müteakip, tutma kuvveti denetleyicisi olarak iki yönlü denetimin değişik bir uygulaması incelenmiştir. İki yönlü denetim için hassasiyet arttırımı üzerine çalışılmış ve bu bağlamda daha iyi hız, ivme ve bozucu etmen kestirimi yapabilecek yeni bir fonksiyonel gözlemci önerilmiştir. Tezin ikinci yarısında, zaman gecikmeli iki yönlü denetim üzerinde yoğunlaşmıştır. Bu amaçla denetleyici tasarımı, pozisyonu ve kuvveti ayrı döngülerde içerecek şekilde yapılmıştır. Zaman gecikmeli pozisyon denetimi için, daha önceden önerilmiş olan, üzerine PD denetleyicileri eklenmiş iletişim bozucu etken denetleyicisi kullanılmıştır. Serbes hareketin dışında, çevre ile etkileşim hareketi yaparken gözlemlenen pozisyon

iraksaması analiz edilmiş ve bunun önün geçmek için bir model takip denetleyicisi önerilmiştir. Zaman gecikmeli kuvvet denetimi için öncelikle bir yerel denetleyicinin tepkisi analiz edilmiştir. Sistem şeffaflığını arttırmak için, gecikmeli köle kuvvetinin yerine köle ortamının çevre parametrelerinin kullanılması önerilmiştir. Bu yapıda çevre katılığının kestirimi bir endirek uyarlamalı denetleyici sayesinde yapılmıştır. Tez boyunca incelenen yapıların tamamı tek serbestlik dereceli efendi ve köle robotlardan oluşan bir sistemde denenmiştir. Önerilen yöntemlerde zaman gecikmeli ve gecikmesiz iki yönlü denetleyiciler için yapılan katkılar deneysel olarak da kanıtlanmıştır.

## **Acknowledgements**

I would like to express my deepest gratitude to my thesis advisor Prof. Dr. Asif Sabanovic, who, with an unbelievable experience and with an endless patience shaped my way in this research. His continuous encouragement and help made me overcome all the problems I faced during my master study. He though me how to be brave and creative when talking about research and I will be recalling his thoughts at every instant of my future academic career.

It is a pleasure for me to give my very special thanks to Dr. Güllü Kızıldaş Şendur and Dr. Kürşat Şendur for their sincere help and support in shaping my academic career and for their valuable efforts in supporting my very first research experiences. They were the first people who opened my way through an academic career for my future.

I would also like to express my debt of gratitude to Dr. Kemalettin Erbatur, Dr. Ahmet Onat and Dr. Volkan Patođlu for their contributions on my undergraduate education. I also want to express my thanks to Dr. Erkey Savař in accepting to be a member of my thesis defence jury.

I am indebted to my friends Duygu Sanaç, Meriç Köselers and Veysel Durur for their continuous friendship and assistance in every difficult phase of my social life during my master.

I would like to acknowledge TUBITAK-Bideb for the financial assistance they provided me with, during the research of this thesis.

Finally, I would like to give my very special thanks to my mother Nurten, my sisters Selen and Yelin and my father Arif for making me the one I am. Especially my father, by drawing my entire way to success throughout all my educational and intellectual life, was the greatest assistance I ever had. I will be pleased to dedicate this thesis to him.



# Contents

<b>1</b>	<b>Introduction</b>	<b>1</b>
1.1	Bilateral Control . . . . .	1
1.2	Problem Definitions . . . . .	5
1.2.1	Bilateral Control Problem . . . . .	5
1.2.2	Time Delay Problem . . . . .	6
1.2.3	Scaling Problem . . . . .	7
1.2.4	Changing DOF Problem . . . . .	8
1.3	Literature Survey . . . . .	10
1.4	Contribution of the Thesis . . . . .	14
<b>2</b>	<b>Bilateral Control without Delay</b>	<b>16</b>
2.1	Preliminary Notes . . . . .	18
2.1.1	System Definition . . . . .	18
2.1.2	Disturbance Observer (DOB) and Acceleration Control	19
2.1.3	Reaction Force Observer (RFOB) . . . . .	20
2.1.4	Experimental Setup . . . . .	22
2.2	Bilateral Controller . . . . .	24
2.2.1	Position Control . . . . .	24
2.2.2	Force Control . . . . .	25
2.2.3	Overall Controller . . . . .	26
2.2.4	Experimental Results . . . . .	27
2.3	A Case Study: Grasping Force Controller . . . . .	30
2.3.1	Formulation of Dynamic Grasping Problem . . . . .	30
2.3.2	Position Control . . . . .	32
2.3.3	Force Control . . . . .	33

2.3.4	Overall Controller . . . . .	34
2.3.5	Experimental Results . . . . .	36
2.4	Performance Improvement . . . . .	39
2.4.1	System Description . . . . .	39
2.4.2	Observer Construction . . . . .	42
2.4.3	Experimental Results . . . . .	47
<b>3</b>	<b>Bilateral Control with Time Delay</b>	<b>51</b>
3.1	Position Control Under Time Delay . . . . .	53
3.1.1	Problem Definition . . . . .	53
3.1.2	Observer and Controller Construction . . . . .	54
3.1.3	Experimental Results . . . . .	59
3.1.4	Additional Compensation for Environment Contact . .	62
3.1.5	Experimental Results . . . . .	66
3.2	Force Control Under Time Delay . . . . .	68
3.2.1	Local Force Controller . . . . .	69
3.2.2	Estimated Force Control with Environment Adaptation	70
3.2.3	Experimental Results . . . . .	72
<b>4</b>	<b>Conclusion &amp; Future Works</b>	<b>74</b>

## List of Figures

1.1	Illustration of actual bilateral system and its ideal representation	2
2.1	Structure of Disturbance Observer . . . . .	20
2.2	Structure of the Reaction Force Observer . . . . .	21
2.3	Picture of the experimental setup . . . . .	23
2.4	Block diagram of bilateral control structure . . . . .	27
2.5	Bilateral Control Tracking Responses . . . . .	28
2.6	Bilateral Control Error Responses . . . . .	29
2.7	Representative drawing of the grasping task . . . . .	30
2.8	Block diagram of the grasping controller . . . . .	35
2.9	Position and force response for step force input . . . . .	37
2.10	Position and force response for sine force input . . . . .	37
2.11	Position and force error for step force input . . . . .	38
2.12	Position and force error for sine force input . . . . .	38
2.13	Structure of a motion control system with ideal observer . . . . .	39
2.14	Proposed observer structure . . . . .	41
2.15	Block diagram of functional observer . . . . .	45
2.16	Velocity responses for step velocity reference . . . . .	47
2.17	Velocity responses for trapezoidal velocity reference . . . . .	48
2.18	Acceleration responses . . . . .	49
2.19	Disturbance estimation responses . . . . .	50
3.1	Representative drawing of normal and delayed system . . . . .	51
3.2	Representative drawing network controller . . . . .	58
3.3	Position response for step reference . . . . .	60
3.4	Position response for sine reference . . . . .	60
3.5	Position response for arbitrary reference . . . . .	61

3.6 Tracking error in contact motion . . . . . 63

3.7 Model following controller structure . . . . . 64

3.8 Environment contact motion with the proposed compensation 67

3.9 Compensated and uncompensated tracking errors . . . . . 67

3.10 Block diagram of the local force controller . . . . . 70

3.11 Experimental results of the local force controller . . . . . 70

3.12 Block diagram of the overall controller . . . . . 72

3.13 Adaptive force reconstruction experiment . . . . . 73

## List of Tables

2.1	Parameters of the Overall Bilateral Controller . . . . .	26
2.2	Parameters of the Overall Grasping Controller . . . . .	36
2.3	Parameters of the Functional Observer for Different Configurations . . . . .	46
3.1	Parameters of the Time Delayed Position Controller . . . . .	57

# Chapter I

## 1 Introduction

### 1.1 Bilateral Control

Interest in the ability of mankind to reach remote locations is ever-growing with the improving technology. Bilateral control, targeting to be used for teleoperation, can provide a human operator with the ability of motion in a remote location and the sense of touch from a remote environment. As obvious from its name, teleoperation (sometimes also referred as telemanipulation) extends human capability to manipulating objects at a distance by providing the operator with similar conditions as those at the remote location. In the general structure, a human operator manually controls a master device (i.e. master system or master robot) and a slave device (i.e. slave system or slave robot) is supposed to track the motion commanded to master device. On the other hand, the master system is supposed to react the human operator with an equal force to the one arising due to interaction of slave system with the remote environment. The word "bilateral control" naturally stands for the task of controlling positions and forces together. This situation is usually illustrated as if there is virtual solid connection between

the master and slave system. A depiction of the described structure can be found Figure 1.1.

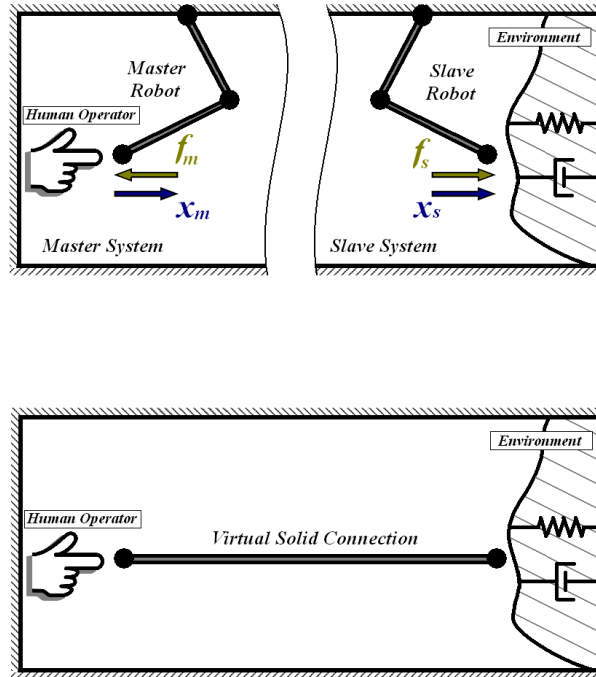


Figure 1.1: Illustration of actual bilateral system and its ideal representation

The control theoretic performance evaluation of bilateral teleoperation systems can be made with respect to two common measures [3].

- **Stability:** The ability to maintain closed loop stability of the controller regardless of the motion of operator or the response of the environment. A teleoperation system should first prove to be stable for real purpose application.
- **Transparency:** A measure, which shows the ability of the the controller to transfer operator motion and environment forces to the remote side and operator respectively. Perfect transparency is achieved when

human operator feels exactly the same forces created by the remote environment and remote system makes exactly the same motion imposed by the human operator.

Following those definitions, an ideal bilateral system can be described as one that can provide stable operation under perfect transparency. There are many areas where bilateral control can effectively be used. Some examples related to the application range of bilateral teleoperation systems can be given as follows:

- Handling hazardous materials: Manipulation of materials that contain nuclear or chemical ingredient or operating in environments where there is risky task for human life (i.e. bomb disposal operations) are good examples where use of bilateral teleoperation effectively decrease the number of casualties.
- Telesurgery: Medical operations that require people with special qualifications can be done from a remote location with bilateral teleoperation. Bringing the remote surgery room to the fingertips of the surgeon would save money, time and effort and would increase the success rate.
- Space robotics: Using teleoperation robots instead of direct human interference will reduce the costs and risks of assembly, maintenance and repair tasks in outer space operations.
- Micro-nano parts handling: Bilateral teleoperation can be used to carry out tasks in micro or nano sizes. Handling and transportation of micro-nano components and assembly in the small scale can be feasible with a correct scaling of motion and/or forces in bilateral control.



- New generation entertainments: Remote controlled game consoles that also include force feedback can open a totally new generation of entertainment area. Bilateral teleoperation can enable a student in China play tennis in real time with a professor in Latin America.

## 1.2 Problem Definitions

Since the very first existence of the idea to have control on bilateral exchange of force and position information, researchers encountered several serious problems. Although the early research trend in bilateral control was mostly concentrated on the time delay problem [49], nowadays, with the advances in micro world and high-tech production capabilities, scientists also investigate the problems of scaling and changing degree of freedom (DOF) in bilateral teleoperation systems. In the following subsections, mathematical formulation of those problems are presented. First, the fundamental problem in bilateral control is shown. Following this, mathematical formulation of the above mentioned three active research topics are introduced.

### 1.2.1 Bilateral Control Problem

As mentioned before, the objective of the bilateral control is to provide the slave system track the position reference generated by master system and to provide the master system reflect the forces felt on the slave system. From a mathematical point of view, this problem can be formulated as follows:

$$x_m - x_s = 0 \quad (1)$$

$$f_m + f_s = 0 \quad (2)$$

where,  $x_*$  and  $f_*$  stand for the position response exhibited and net external force felt by the corresponding system (\*) respectively. From this point on, unless otherwise stated, the subscripts  $m$  and  $s$  will denote the quantities that belong to master and slave systems respectively. For the objective described above, instead of positions, one can also use the velocity response and impose

tracking of master system velocity by the slave system. Speaking about variables that represent flow (i.e. velocity) and effort (i.e. force), one can formulate the intermediate transition using the idea of impedances [1]. This way a common transition can be formulated between the master and slave systems as follows

$$\begin{bmatrix} F_m(s) \\ V_m(s) \end{bmatrix} = \begin{bmatrix} H_{11}(s) & H_{12}(s) \\ H_{21}(s) & H_{22}(s) \end{bmatrix} \begin{bmatrix} V_s(s) \\ -F_s(s) \end{bmatrix} \quad (3)$$

where, the matrix in between is called the hybrid impedance matrix [2]. As stated in [3], the ideal operation conditions (i.e. perfect transparency) can be achieved when

$$H(s) \doteq \begin{bmatrix} H_{11}(s) & H_{12}(s) \\ H_{21}(s) & H_{22}(s) \end{bmatrix} = \begin{bmatrix} 0 & 1 \\ 1 & 0 \end{bmatrix} \quad (4)$$

### 1.2.2 Time Delay Problem

In order to realize teleoperation, one needs a network to carry out data exchange with the remote plant. However, it is known that the networks are usually subject to transmission delays. Moreover, due to computational complexity, the network delay can even be augmented in the master and slave controllers. As a result, the system dynamics changes and a time delayed system description comes into picture. For the unilateral formalism (i.e. including only the input delay), such a system can be represented as

$$\begin{aligned} \dot{\mathbf{x}}(\mathbf{t}) &= \mathbf{A}\mathbf{x}(\mathbf{t}) + \mathbf{B}\mathbf{u}(\mathbf{t} - \mathbf{D}) \\ \mathbf{y}(\mathbf{t}) &= \mathbf{C}\mathbf{x}(\mathbf{t}) \end{aligned} \quad (5)$$

where,  $\mathbf{x} \in \mathbb{R}^{n \times 1}$ ,  $\mathbf{u} \in \mathbb{R}^{m \times 1}$  and  $\mathbf{y} \in \mathbb{R}^{r \times 1}$  are the state, input and output vectors respectively. The matrices  $\mathbf{A} \in \mathbb{R}^{n \times n}$ ,  $\mathbf{B} \in \mathbb{R}^{n \times m}$  and  $\mathbf{C} \in \mathbb{R}^{r \times n}$  are called the state transition matrix, input distribution matrix and output matrix respectively. It is very well known that even such an input delayed system can exhibit instable behavior [4], [5], [6]. When there is time delay in both measurement and control (input) (i.e. practical case observed in teleoperation systems), providing stable behavior becomes even more challenging. Without loss of generality, a time delayed bilateral control system can be given by

$$\begin{aligned} x_s(t) &= g\{x_m(t - D_c), f_m(t - D_c), f_s(t)\} \\ x_m(t) &= g\{x_s(t - D_m), f_s(t - D_m), f_m(t)\} \end{aligned} \quad (6)$$

where  $D_c$  and  $D_m$  stand for the time delays in the control and measurement channels respectively. Usually, time delays are not constant and they exhibit a time-varying behavior. Bilateral teleoperation under time delay can be achieved when a controller satisfies equations (1) and (2) with the constraints given in (6). This is still an open problem.

### 1.2.3 Scaling Problem

With the recent advances in micro-nano technology, it became possible to move robotic manipulation into the small scale operations (i.e. MEMS products or cell injection processes). Improvements on small scale manipulability revealed the path for using bilateral teleoperation in micro-nano applications. In order to have this capability, one has to make sure that there exists a correct scaling for forces and positions, so that the physical environment in

micro scale can be transformed to magnitudes realizable by human operators. The mathematical formulation of position and force scaling can be given by

$$\begin{aligned}x_m - \alpha x_s &= 0 \\f_m + \beta f_s &= 0\end{aligned}\tag{7}$$

where coefficients  $\alpha$  and  $\beta$  determine the scaling ratio between positions and forces respectively. In the impedance representation, the hybrid matrix for an ideal scaled bilateral teleoperation system can be given by

$$H(s) = \begin{bmatrix} 0 & \beta \\ \alpha & 0 \end{bmatrix}\tag{8}$$

Practical realization of scaled bilateral teleoperation can be found in [7], [8] and [9]. Some recent and interesting studies even integrate the achievements in atomic force microscopy (AFM) with bilateral teleoperation to utilize the haptic feeling of atomic surfaces [10], [11].

#### 1.2.4 Changing DOF Problem

For some specialized tasks like telesurgery operations, one might need to have two different kinematic configurations in master and slave systems. The changing configuration is usually structured for the particular type of application and may possibly lead to master and slave robots having different degrees of freedom. Under such a condition, the dimensions of forces and positions exceed two and the resultant system is usually referred as a multilateral system [12], [13]. For systems with different DOF, the bilateral teleoperation problem can be re-formulated under the context of multilateral

control as follows

$$\begin{aligned} \sum_{i=1}^k \mathbf{x}_m^i - \sum_{j=1}^p \mathbf{x}_s^j &= 0 \\ \sum_{i=1}^k \mathbf{f}_m^i + \sum_{j=1}^p \mathbf{f}_s^j &= 0 \end{aligned} \quad (9)$$

where,  $\mathbf{x}_*^i$  and  $\mathbf{f}_*^j$  represent the  $i^{th}$  position vector and  $j^{th}$  force vector of the corresponding system (\*) respectively. Here it is assumed that the master system is  $k$ -dimensional and the slave system is  $p$ -dimensional. Some examples of the applications of multilateral control include haptic training mechanisms for disabled patients [14] and grasping controllers for the robotic systems [15].

### 1.3 Literature Survey

Historically, the idea of bilateral control started as early as 1940s and 1950s when the first mechanical master-slave manipulator was introduced [16]. During 1960s and 1970s, scientists started to investigate force reflection under the effect of delays [17], [18]. Around the mid 1980s, more advanced control theoretic methods such as Lyapunov-based analysis started to appear [19]. Following the advances in the network theory in late 1980s, control schemes involving hybrid approaches [20] and impedance representation [21] was introduced for teleoperation systems. First stable time delayed teleoperation was achieved when Anderson and Spong used the passivity theory to guarantee stability of the closed loop time delay system [22]. Unfortunately, such an energy based approach lacks in providing satisfying transparency, which is the second evaluation of success in teleoperation systems [3]. Moreover, the proposed passivity method was constrained with applications involving constant and apriori known time delay. The idea to use scattering theory instead of direct power transfer through network could overcome the interference of wave reflections and result in better closed loop dynamics. Originating from this point, Niemeyer and Slotine proposed wave variables which revealed a good solution to provide both stability and transparency under constant time delays of any magnitude [23], [24].

For scenarios including time varying delay in bilateral teleoperation, there is still not a fully satisfying solution. For unpredictable communication delay, modified wave variables is proposed to provide necessary stability in force reflecting teleoperation [25]. Modified wave variables is also shown to improve the force tracking performance in teleoperation systems [26]. Yokokohji et al improved the modified wave variables method to minimize the performance

degeneration of bilateral teleoperation under time varying communication delay [27]. Some other studies were also carried out to increase the performance of wave variables. In their study, Munir and Book used a modified Smith Predictor and a Kalman Filter to add predictive characteristics to wave based teleoperation. Their work was also important in the experimental sense since it first demonstrated the possibility of intercontinental teleoperation [28]. A detailed formalism of wave based prediction and application of wave variables to unknown time delay can also be found in [29]. In either cases, however, relation between the magnitudes of time delay and system time constant is crucial in determining the overall performance of the system. Other than wave variables, Ryu and Preusche modified the previously proposed two port time domain passivity approach [30] to obtain stable bilateral teleoperation under time varying delay [31]. In a recent study, additional position controllers are used to provide steady state position and force tracking for passivity controllers [32]. Moreover, advantages of employing local force feedback for enhanced stability and performance was investigated in [33].

Several other studies have also been carried out to apply methods from the context of control theory. In [34], an adaptive law for the automatic tuning of model time delay in a Smith Predictor is implemented. The new structure is shown to increase the performance of Classical Smith Predictor via decreasing the sensitivity to modeling errors. Another adaptation scheme was considered in [35] to increase the transparency of the previously proposed impedance reflecting bilateral teleoperation [36]. In their study, Slama et al implemented the generalized predictive control structure to enhance the performance of control based on delayed force feedback [37]. An optimal strategy based on  $H_\infty$  control and  $\mu$ -synthesis is applied to optimize performance specifications



in time delayed bilateral control [38].

Besides the classical methods related to power transfer and scattering theory, recently proposed Communication Disturbance Observer (CDOB) seems to bring a conclusion to stability problem originated from variable delay of any magnitude [39], [40]. CDOB offers a framework for the application of disturbance observer for the systems with constant and/or time varying delay. Ohnishi et. al. made use of CDOB to realize bilateral teleoperation [41]. Although it is both theoretically and experimentally verified that CDOB is effective to stabilize a network delayed motion control system, position convergence of slave is degenerated especially when the initial conditions of master and slave systems are different. In order to enforce position convergence, Sabanovic et. al. proposed an observer-predictor structure utilizing a PD convergence controller along with CDOB [42], [43].

Quantitative and analytical comparison of the existing methods for time delay problem can be found in [46] and [47]. For more detailed information, reader is referred to the historical survey given in [48].

Besides the time delay problem, recently, scientists started to specialize on scaling issue of bilateral teleoperation. Some early studies addressing the scaling phenomena in bilateral teleoperation can be found in [53] and [54]. The former one investigates the possibility of micro-nano scale manipulation while the latter one makes a general theoretical analysis on scaling of any magnitude. In [55], a performance measurement for teleoperation in microsurgery is presented while the stability and transparency issues for scaled teleoperation systems can be found in [56]. Advances in atomic force microscopy augmented the interest in the feasibility of haptic feeling from an atomic structure. Studies including the AFM based force measurement from

atomic structures ([57], [11]) and nanorobotics [58] are still among the hot research topics of scaled bilateral teleoperation. A recent investigation of scaled bilateral control based on a sliding mode approach can be found in [70].

Improvements in the context of multilateral control came into picture with growing interest on practical applications. This is because many real systems (i.e. surgery robots, rehabilitation robots) require certain constraints on the end effector (i.e. slave side) while a more flexible design on the operator tool (i.e. master side) improves operation quality. Some recent approaches to the multilateral control problem include the modal decomposition approach [59], [60]. Another satisfying solution comes with the use of query matrices [61], [62]. In [63], an adaptive nonlinear controller was implemented to realize multilateral control. Other examples of multi-robot teleoperation can be found in [64] and [65]. For a complete formulation of the bilateral teleoperation along with the analysis and solutions to the various problems in the context of motion control, reader is referred to [52].

## 1.4 Contribution of the Thesis

In the context of this thesis, following studies are carried out:

- Implementation of bilateral control based on DOB  
Originating from the fundamentals of disturbance observer and robust acceleration control, analysis and implementation of a previously shown bilateral control scheme is done.
- Analysis and implementation of a new grasping control scheme  
Using a similar idea to that of the bilateral control and by creating the corresponding functional relationship between two coupled systems it is shown that same DOB based approach can also be used for dynamic grasping of objects with known parameters.
- A novel functional observer is proposed and implemented  
In order to improve the overall system performance, the ways to have a better observer is studied. For estimation, instead of using position response and approximations of improper transfer functions in the observer, an new structure is proposed that makes use of current input and strictly proper transfer functions.
- Analysis and implementation of network position controller  
In order to realize stable position control under time delay, a previously proposed observer & controller structure is implemented. Proof of stability is also included in the derivation.
- Additional compensation for contact motion  
In the context of time delayed position control, contact motion is also experimented. It is observed that the output of the slave system cannot

track master reference under contact motion. This problem is analyzed mathematically and a solution is proposed that makes use of a virtual plant in a model following control structure.

- A new method for delayed force control

In order to obtain a full bilateral control with time delay, inclusion of force control in the overall loop is investigated. For the force control under time delay, a new approach is proposed and implemented that makes use of the estimated environment stiffness for force reconstruction. Estimation of the stiffness is made via an indirect adaptive control algorithm.

# Chapter II

## 2 Bilateral Control without Delay

In this chapter the analysis and design of bilateral control is investigated with the exclusion of time delay effect. The structure implemented here was originally proposed in [50]. The main logic behind the analyzed structure is based on the preservation of nominal system (i.e. double integrator plant) that can accept acceleration references and controller derivation in the acceleration dimension. For the on going investigation, extensive use of robust motion control and acceleration control is made.

In order to come up with the a nominal plant structure (i.e. a double integrator plant), one has to make sure that all the undesired effects (i.e. disturbances) acting on the system are taken away. For the realization of disturbance rejection, Disturbance Observer (DOB) is implemented. This way, both master and slave systems are made robust with respect to disturbances. Following this achievement, controller derivation for position and force servoing is made to generate the necessary acceleration references for the plants. Since disturbance rejection and robust motion control lies in the core of the design, in the first section of this chapter, the preliminary notes about the details of DOB and acceleration control are presented.

During the implementation, sensorless force measurement is made using

Reaction Force Observers (RFOB). In order to have a complete analysis, the derivation of RFOB is also included in the preliminary notes section.

Moreover, since all of the analysis provided in the context of this thesis are also experimentally validated, in the last part of the preliminary notes the experimental setup is described.

## 2.1 Preliminary Notes

### 2.1.1 System Definition

In the following parts, analysis and derivations are made over a one DOF motion control control system for the sake of simplicity. The results obtained can then be generalized to MIMO systems. The plant dynamics of a single DOF motion control system can be given by

$$M_n \ddot{x}(t) = \tau_c(t) - \tau_{dis}(t) \quad (10)$$

where,  $M_n$ ,  $\tau_c(t)$  and  $\tau_{dis}(t)$  represent the nominal plant inertia, input torque and disturbance torque acting on the plant respectively. The input torque to the system can be modeled as a scaler multiple of the input current and nominal torque constant (i.e.  $\tau_c(t) = K_n i_c(t)$ ) [66]. Substituting this into (10) gives the following

$$M_n \ddot{x}(t) = K_n i_c(t) - \tau_{dis}(t) \quad (11)$$

In equation (11), it is assumed that the term  $\tau_{dis}(t)$  lumps all undesired effects, including the viscous friction ( $B(x, \dot{x})$ ), deviations from the nominal values for torque constant ( $\Delta K_n$ ) and inertia ( $\Delta M_n$ ), gravitation ( $G(x)$ ) and all other non-modeled external torques ( $\tau_{ext}$ ). This way the model of disturbance torque can be given as

$$\tau_{dis}(t) = \Delta M_n \ddot{x}(t) + \Delta K_n i_c(t) + B(x, \dot{x}) \dot{x}(t) + G(x(t)) + \tau_{ext}(t) \quad (12)$$

### 2.1.2 Disturbance Observer (DOB) and Acceleration Control

For the dynamic system given in (11), removing the disturbance torque is of crucial importance for the applicability of acceleration control. To estimate and cancel the disturbance acting on the system, a disturbance observer (DOB) can be realized [67]. The internal structure of disturbance observer includes a low pass filter. Having a high filter gain, disturbance observer can be designed to cancel the disturbance torque as quickly as possible. The estimated disturbance can be obtained from the velocity response  $\dot{x}$  and current input  $i_c$  of the system and be fed back to the plant. The velocity response is calculated from the position data using a velocity observer. However, although in many applications disturbance observer can effectively increase the robustness of a system, due to the low pass filter used in the structure, the disturbance might not always be fully compensated, which in turn leads to imperfections in estimation. Having this in mind, the motion control system given in (11), with the addition of disturbance observer, can be re-formulated as follows

$$M_n \ddot{x}(t) = K_n i_c(t) - \delta \tau_{dis}(t) \quad (13)$$

where,  $\delta \tau_{dis}(t) = \tau_{dis}(t) - \hat{\tau}_{dis}(t)$  stands for the disturbance estimation error. Under perfect disturbance cancelation the plant is desired to behave like a double integrator system. But because of the imperfection on DOB output, the estimation error is also double integrated. So, without additional control loop the velocity and position responses can diverge from the corresponding



references, which can be modeled as

$$\begin{aligned}\dot{x}^{res}(t) &= \dot{x}^{ref}(t) + \int_0^t \delta\tau(\zeta)d\zeta \\ x^{res}(t) &= x^{ref}(t) + \int_0^t \int_0^t \delta\tau(\zeta)d\zeta d\psi\end{aligned}\quad (14)$$

where, the superscripts *ref* and *res* represent the reference and response of the corresponding variable respectively. The structure of disturbance observer is given in Figure 2.1.

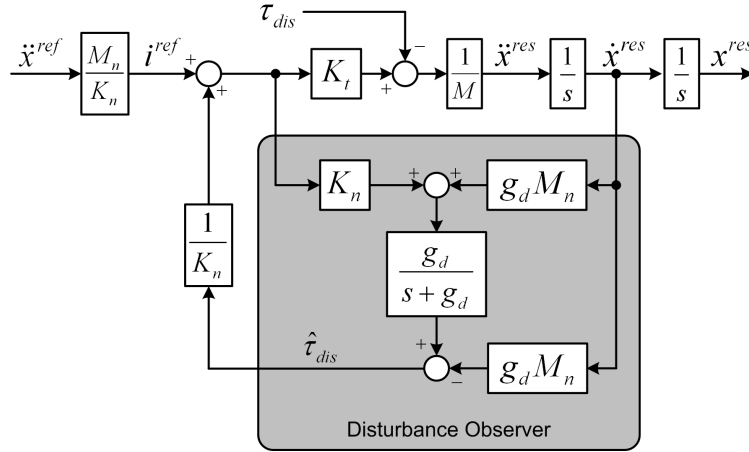


Figure 2.1: Structure of Disturbance Observer

### 2.1.3 Reaction Force Observer (RFOB)

In the preceding discussion, the estimated disturbance torque is fed back to the system to provide robust motion control in the acceleration framework. However, when an accurate identification of the system exists, by feed forwarding all the known torques, one can also estimate the external torque acting on the system [68]. Mathematically, the external torque acting on the

system can be estimated as:

$$\hat{\tau}_{ext} = \{\tau_{dis} - (B(x, \dot{x})\dot{x} + G(x))\} \frac{g_r}{s + g_r} \quad (15)$$

Here it is assumed that the viscous friction coefficient  $B$ , the effect of gravity  $G$ , the nominal inertia  $M_n$  and the nominal torque constant  $K_n$  are known beforehand and the fluctuation of inertia and torque constant are negligibly small (i.e.  $\Delta K_n, \Delta M_n \approx 0$ ). Like disturbance observer, the estimation accuracy depends on the filter gain  $g_r$ . A depiction of this observer (so called as Reaction Force Observer) is given in Figure 2.2. In this structure, since the

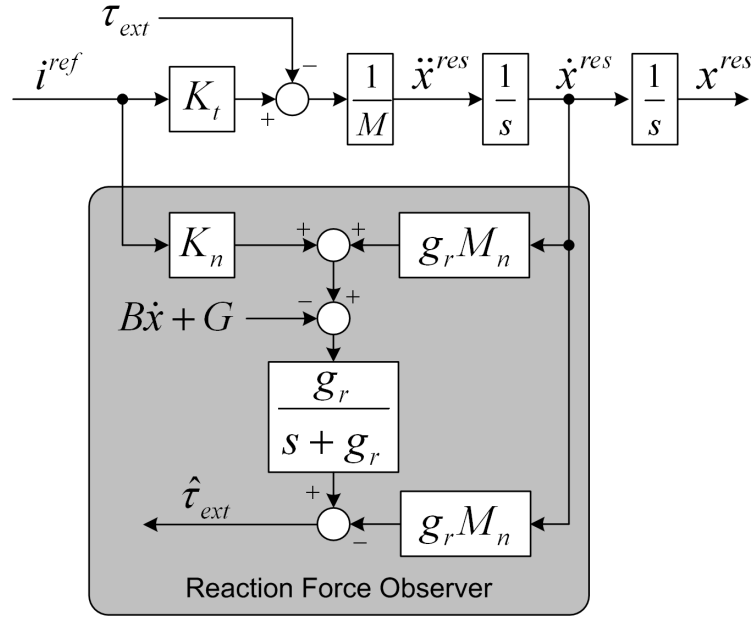


Figure 2.2: Structure of the Reaction Force Observer

force estimation is made using the input current and velocity measurement, a very fast force estimation response can be obtained using a high gain low pass filter. However, limitations on the filter gain also introduce the bandwidth

limitations in the force estimation which was analyzed in [68].

#### 2.1.4 Experimental Setup

Illustration of all of the material presented in this thesis is made by verification on an experimental system consisting of linear motors. Two Hitachi-ADA series linear AC motors and drivers were used as the experimental platform. In that sense, first the solid drawings of the setup was made and it was produced accordingly. Following this, electrical connections are made in order to drive the system in current control mode. Noise reduction is achieved by the use of printed circuit boards.

The linear motors had Renishaw RGH41 type incremental encoders with  $1\mu m$  resolution. So, the overall system precision was around  $1\mu m$ . MATLAB-Simulink environment along with Matlab-Executable (MEX) subroutines was used as the implementation software and real time processing was enabled by a D-Space DS1103 card. A sampling frequency of 1KHz was used for the DSP board. Force measurement was handled by the reaction force observer structure presented in the previous section. A picture of the experimental setup is provided in Figure 2.3.

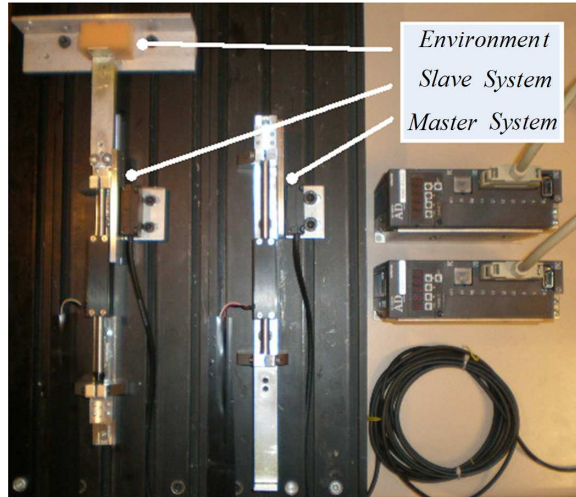


Figure 2.3: Picture of the experimental setup

Talking about the overall system performance, the linear motors are capable of exerting a maximum of  $12N$  force which is enough (i.e. easy to realize by the human operator) for many applications. The static friction on both systems was approximately around  $0.5N$ . During experiments, the linear motors were used in different configurations according to the targeted objective.

## 2.2 Bilateral Controller

Bilateral controller can be designed to satisfy the conditions given in equations (1) and (2). Assuming the measurements of positions, velocities and forces from the master and slave sides are available, and assuming both plants have DOBs integrated, design can be made to obtain acceleration references  $\ddot{x}_m^{ref}$  and  $\ddot{x}_s^{ref}$  for the corresponding system [50], [52].

### 2.2.1 Position Control

Using the position and velocity measurements of master and slave systems, one can define the tracking error as a linear combination of errors in position and velocity tracking as follows,

$$\varepsilon_x = C_1(\dot{x}_m - \dot{x}_s) + C_2(x_m - x_s) \quad (16)$$

In order to impose the exponential decay for this error, the following error dynamics can be implemented,

$$\begin{aligned} \dot{\varepsilon}_x &= -K_x \varepsilon_x \\ C_1(\ddot{x}_m - \ddot{x}_s) + C_2(\dot{x}_m - \dot{x}_s) &= -K_x \{C_1(\dot{x}_m - \dot{x}_s) + C_2(x_m - x_s)\} \end{aligned} \quad (17)$$

where,  $K_x$  defines the exponential decay rate of the error. In equation (17), a transformation can be made and the difference between the master and slave accelerations can be renamed as the differential mode acceleration (i.e.  $\ddot{x}_{dif} = (\ddot{x}_m - \ddot{x}_s)$ ). Following the transformation, this equation can be rearranged to give the reference differential acceleration to drive the acceleration controlled

plants

$$\ddot{x}_{dif}^{ref} = \frac{1}{C_1} \{(-K_x C_1 - C_2)\dot{x}_{dif} - (K_x C_2)x_{dif}\} \quad (18)$$

### 2.2.2 Force Control

Under the assumption that the disturbances acting on the systems are rejected with DOBs, one can assume that the force measurement is a scalar multiple of the acceleration response. Having this in mind, the force measurement of identical master and slave systems both with inertia  $M_n$  can be expressed as follows

$$\begin{aligned} F_m &= M_n \ddot{x}_m \\ F_s &= M_n \ddot{x}_s \end{aligned} \quad (19)$$

Just like differential mode, another transformation can be made for (2) and the sum of the master and slave accelerations can be renamed as the common mode acceleration (i.e.  $\ddot{x}_{com} = (\ddot{x}_m + \ddot{x}_s)$ ). The constraint given in equation (2) imposes the sum of forces be equal to zero (i.e.  $M_n(\ddot{x}_m + \ddot{x}_s) = M_n \ddot{x}_{com} = 0$ ). In order to satisfy this error condition, one can formulate a proportional control for the force control loop and write the reference common mode acceleration as follows

$$\ddot{x}_{com}^{ref} = K_f \varepsilon_{com} \quad (20)$$

where the error in common mode is given as the difference between zero reference and common mode acceleration response (i.e.  $\varepsilon_{com} = 0 - \ddot{x}_{com}^{res}$ ). Rearranging (20) and inserting back the forces instead of master and slave accelerations, one can come up with the following common mode reference

acceleration

$$\ddot{x}_{com}^{ref} = -\frac{K_f}{M_n}(F_m + F_s) \quad (21)$$

### 2.2.3 Overall Controller

Now we have the common and differential mode accelerations to provide force and position tracking of the bilateral system. The only remaining thing is a transformation back to the master and slave acceleration references. Although the sources of reference accelerations for force control (i.e. common mode) and position control (i.e. differential mode) are different, due to the superposition principle, they can be algebraically added. Using the definitions of common and differential mode accelerations, one can write the following back transformation

$$\begin{aligned} \ddot{x}_m^{ref} &= \frac{1}{2}(\ddot{x}_{com}^{ref} + \ddot{x}_{dif}^{ref}) \\ \ddot{x}_s^{ref} &= \frac{1}{2}(\ddot{x}_{com}^{ref} - \ddot{x}_{dif}^{ref}) \end{aligned} \quad (22)$$

The block diagram of this control scheme is depicted in Figure 2.4 and a summary content of gains  $K_1$ ,  $K_2$  and  $K_3$  can be found in the table given below

$K_1$	$K_2$	$K_3$
-----	-----	-----
$\frac{-K_x C_2}{C_1}$	$\frac{(-K_x C_1 - C_2)}{C_1}$	$\frac{-K_f}{M_n}$

Table 2.1: Parameters of the Overall Bilateral Controller

The performance of the controller depends on the gains selected and the structure of DOB used. Position and velocity gains can be relatively high, however, gain of the force control loop should be more carefully selected since high gain can cause instability of the system. Besides controller gains, it is important to have a fast disturbance rejection on both master and slave sides. So, the filter of the DOB for the plants should be selected with the highest possible gains.

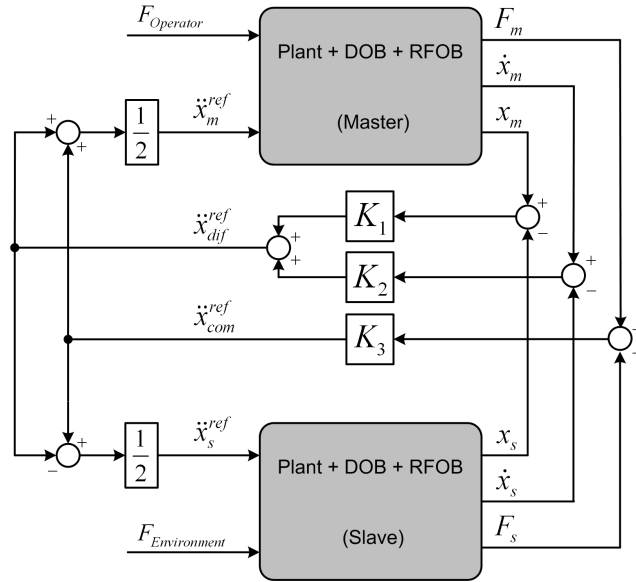


Figure 2.4: Block diagram of bilateral control structure

## 2.2.4 Experimental Results

The depicted controller is implemented on the before-mentioned experimental setup. For the experiment, the master system reference is generated by a human operator and the slave system is allowed to exhibit both free and contact motion. In that sense, environment in the slave side is located after a certain distance of free motion. The results of the experiment are given



in Figure 2.5. It is also clear from this figure that the master and slave positions and forces are obeying the bilateral control constraints given in (1) and (2). The force and position tracking errors, given in Figure 2.6, are negligibly small compared to the references. It should be noted here that the environment at the slave side is located at 7 mm away from the initial conditions. So, the position and force tracking response after slave exceeds this point represents the contact motion of the controller. Finally, as obvious from the graphs, tracking response for the contact motion is worse than the responses obtained for free motion. This is basically due to the imperfections of the DOB in eliminating the disturbances resulting from an environment contact, and is analyzed in detail in the following chapter.

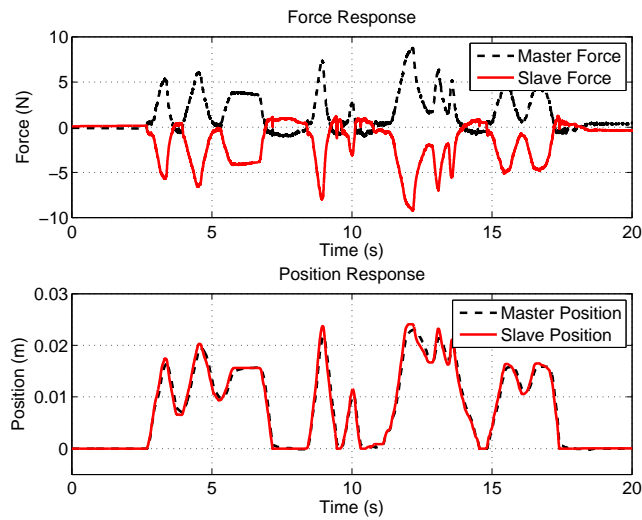


Figure 2.5: Bilateral Control Tracking Responses

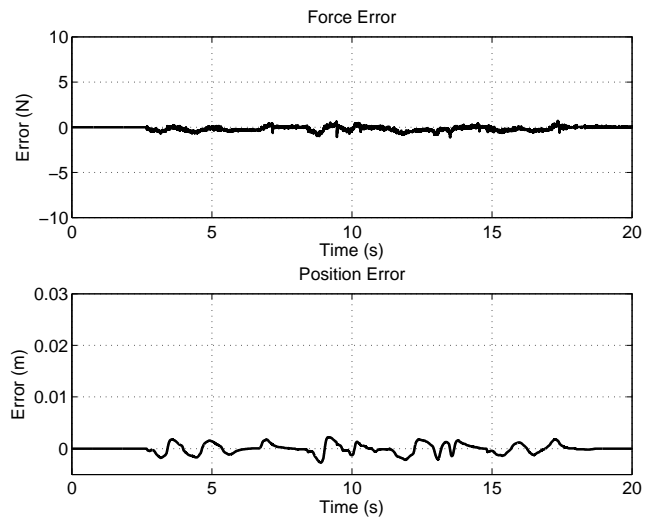


Figure 2.6: Bilateral Control Error Responses

## 2.3 A Case Study: Grasping Force Controller

### 2.3.1 Formulation of Dynamic Grasping Problem

In the following analysis, it is assumed that the grasping operation is carried out by two identical actuators. By establishing the correct functional relationship between the master and slave robots, one can formulate the control objective in force and position loops for dynamic grasping control [52]. Due to the coupled control goal of position and force, without loss of generality, one can convert the dynamic grasping problem into a bilateral control problem. Figure 2.7 shows a drawing of the system under scope. Here,  $F_m$  and  $F_s$  represent the reaction forces on the master and slave actuators respectively. On the other hand,  $x_{mc}$  and  $x_{sc}$  represent the master and slave contact coordinates to the non-deformed object while  $x_{md}$  and  $x_{sd}$  represent the master and slave contact coordinates to the deformed object respectively. Finally,  $x_o$  indicates the position of the center of gravity of the object. During grasp-

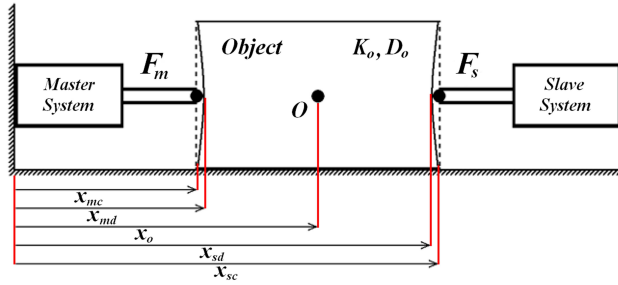


Figure 2.7: Representative drawing of the grasping task

ing, since the inertia of the deformed piece of the object is very small, one can omit the inertial forces of deformation. Moreover, it is assumed that the stiffness ( $K_o$ ) and damping ( $D_o$ ) of the object to be grasped is known a priori. Following these assumptions, the reaction forces of the master and

slave actuators can be given as follows:

$$\begin{aligned} F_m &= K_o(x_{mc} - x_{md}) + D_o(\dot{x}_{mc} - \dot{x}_{md}) \\ F_s &= -K_o(x_{sc} - x_{sd}) - D_o(\dot{x}_{sc} - \dot{x}_{sd}) \end{aligned} \quad (23)$$

Since sum of the master and slave forces gives the total force exerted on the object, one can write down the grasping force as follows:

$$F_g = F_m + F_s$$

$$F_g = K_o(x_{mc} - x_{md}) + D_o(\dot{x}_{mc} - \dot{x}_{md}) - K_o(x_{sc} - x_{sd}) - D_o(\dot{x}_{sc} - \dot{x}_{sd})$$

Using a coordinate transformation it is possible to rewrite this equation in terms of the deformations on the master and slave sides as follows,

$$x_m = x_{mc} - x_{md} \quad (24)$$

$$x_s = x_{sc} - x_{sd} \quad (25)$$

hence the grasping force can be simplified to

$$F_g = K_o(x_m - x_s) + D_o(\dot{x}_m - \dot{x}_s) \quad (26)$$

Besides the force, since the target is to control the grasped object under dynamic behavior, one should define a target position to control. Without loss of generality one can select the center of gravity of the object as the target position to be controlled. For a uniform object the center of gravity will be the mid point of master and slave coordinates and thus can be written

as:

$$x_o = \frac{(x_m + x_s)}{2} \quad (27)$$

Moreover, since both master and slave system can have integrated DOBs, one can assume that master and slave systems can perform tracking of the acceleration references. Now, following the disturbance rejection assumption and using the definitions above, the dynamic grasping problem can be transformed to finding the master and slave acceleration references ( $\ddot{x}_m$  and  $\ddot{x}_s$ ) that would satisfy the following equations:

$$x_o^{res} = x_o^{ref} \quad (28)$$

$$F_g^{res} = F_g^{ref} \quad (29)$$

### 2.3.2 Position Control

Following the position tracking objective given in (28), one can write down an augmented position error that also includes the velocity information as follows

$$\varepsilon_x = C(x_o^{ref} - x_o) + (\dot{x}_o^{ref} - \dot{x}_o) \quad (30)$$

where  $C$  is an arbitrary positive constant. Equation (30) can be rearranged to include the master and slave positions using the identity given in (27). Hence the position error becomes

$$\varepsilon_x = C \left( x_o^{ref} - \frac{(x_m + x_s)}{2} \right) + \left( \dot{x}_o^{ref} - \frac{(\dot{x}_m + \dot{x}_s)}{2} \right) \quad (31)$$

In order to obtain an exponentially decaying error, the following dynamics can be imposed on the system

$$\dot{\varepsilon}_x = -K_x \varepsilon_x \quad (32)$$

Substituting the error  $\varepsilon_x$  from (31) and rearranging (32), one can find the summation of master and slave reference accelerations for an exponentially decaying error in position tracking

$$\begin{aligned} \ddot{x}_m^{ref} + \ddot{x}_s^{ref} &= \{2\ddot{x}_o^{ref} + 2(K_x + C)\dot{x}_o^{ref} + 2K_x C x_o^{ref}\} \\ &- \{(K_x + C)(\dot{x}_m + \dot{x}_s) + K_x C(x_m + x_s)\} \end{aligned} \quad (33)$$

Using a similar argument to the bilateral control, one can insert the definition of common mode acceleration term instead of summation of accelerations. Having this in mind and observing that there are similar coefficients, one can rewrite equation (33) as

$$\ddot{x}_{com}^{ref} = 2 \{ \ddot{x}_o^{ref} + K_1 \dot{x}_o^{ref} + K_2 x_o^{ref} \} - \{ K_1 (\dot{x}_m + \dot{x}_s) + K_2 (x_m + x_s) \} \quad (34)$$

where,  $K_1 = K_x + C$  and  $K_2 = K_x C$ .

### 2.3.3 Force Control

Using the definition of grasping force and tracking objective given in (29), one can define the following error in force tracking.

$$\varepsilon_f = F_g^{ref} - K_o(x_m - x_s) - D_o(\dot{x}_m - \dot{x}_s) \quad (35)$$

Since the force reference is smooth and differentiable, one can obtain the dynamics for an exponentially decaying force error as follows

$$\dot{\varepsilon}_f = -K_f \varepsilon_f \quad (36)$$

Substituting the error from (35) and rearranging (36) it is possible to obtain the difference of accelerations that will imply an exponentially decaying error in force tracking

$$\begin{aligned} \ddot{x}_m^{ref} - \ddot{x}_s^{ref} &= \frac{1}{D_o} \left\{ \dot{F}_g^{ref} + K_f F_g^{ref} \right\} \\ &- \frac{1}{D_o} \left\{ (K_f D_o + K_o)(\dot{x}_m - \dot{x}_s) - K_f K_o(x_m - x_s) \right\} \quad (37) \end{aligned}$$

Equation (37), includes the differences of accelerations. Renaming this difference as the differential mode acceleration, and grouping the coefficients, one can finally obtain

$$\ddot{x}_{dif}^{ref} = \left\{ K_3 \dot{F}_g^{ref} + K_4 F_g^{ref} - K_5(\dot{x}_m - \dot{x}_s) - K_6(x_m - x_s) \right\} \quad (38)$$

where  $K_3 = \frac{1}{D_o}$ ,  $K_4 = \frac{K_f}{D_o}$ ,  $K_5 = K_f + \frac{K_o}{D_o}$  and  $K_6 = \frac{K_f K_o}{D_o}$ .

#### 2.3.4 Overall Controller

Just like the bilateral case analyzed in the previous section, once the differential and common mode acceleration references are obtained, the only remaining thing is a back transformation that can be used to acquire independent master and slave acceleration references. Such a transformation was given in equation (22). The block diagram of the final grasping controller is given in Figure 2.8 and a summary of the coefficients used is tabulated in

Table 2.3.4.

Having a look at the general controller structure, one can observe that there are several differences between the bilateral controller and grasping force controller. The most important difference is in the structure of the force control loop. For grasping control, since the reference grasping force and the parameters of the object are a priori known, it is possible to take the derivative of force error. Because of this, the force tracking performance of grasping force is relatively better than that of bilateral control. However, the force control loop of grasping is more sensitive to parameter uncertainties than that of bilateral control.

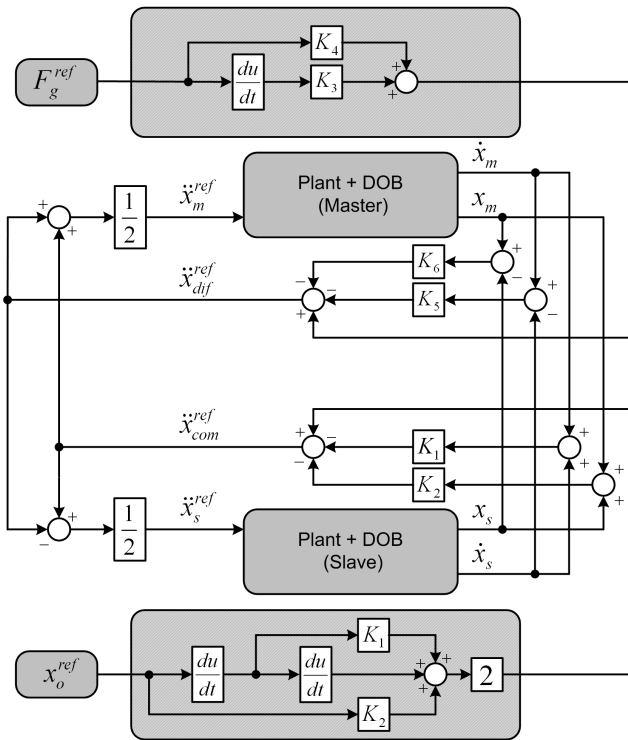


Figure 2.8: Block diagram of the grasping controller



$K_1$	$K_2$	$K_3$	$K_4$	$K_5$	$K_6$
-----	-----	-----	-----	-----	-----
$K_x + C$	$K_x C$	$\frac{1}{D_o}$	$\frac{K_f}{D_o}$	$K_f + \frac{K_o}{D_o}$	$\frac{K_f K_o}{D_o}$

Table 2.2: Parameters of the Overall Grasping Controller

### 2.3.5 Experimental Results

The performance of the investigated structure is tested in experiments. For experiments, master and slave devices are flipped to each other so that they can keep an object in their actuation points. Two different sets of experiments are carried out. For both experiments the reference position for center of gravity was selected as sinus. For force references, on the other hand, in the first set the grasping force reference was selected as a constant whereas in the second set the grasping force reference was also selected as a sinus wave. The results of the experiments are shown in Figure 2.9 and Figure 2.10 for step and sinus force references respectively while the tracking errors for those experiments are given in Figure 2.11 and Figure 2.12.

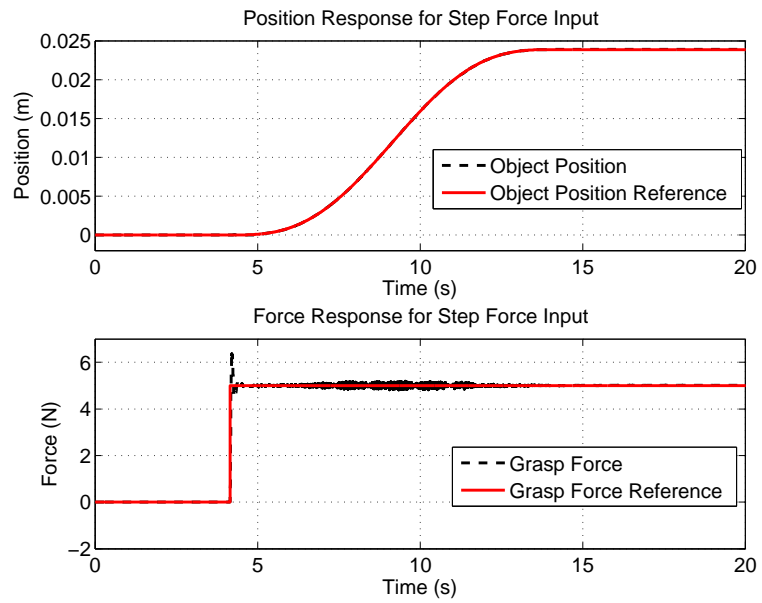


Figure 2.9: Position and force response for step force input

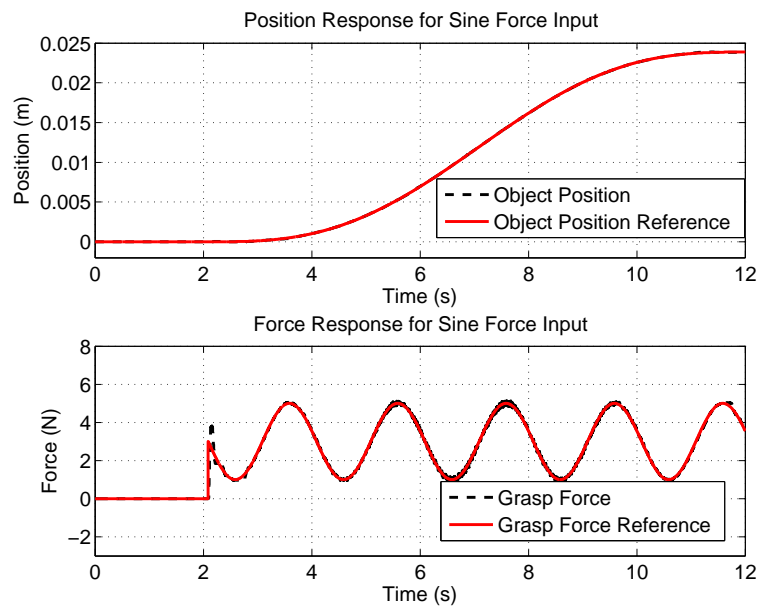


Figure 2.10: Position and force response for sine force input

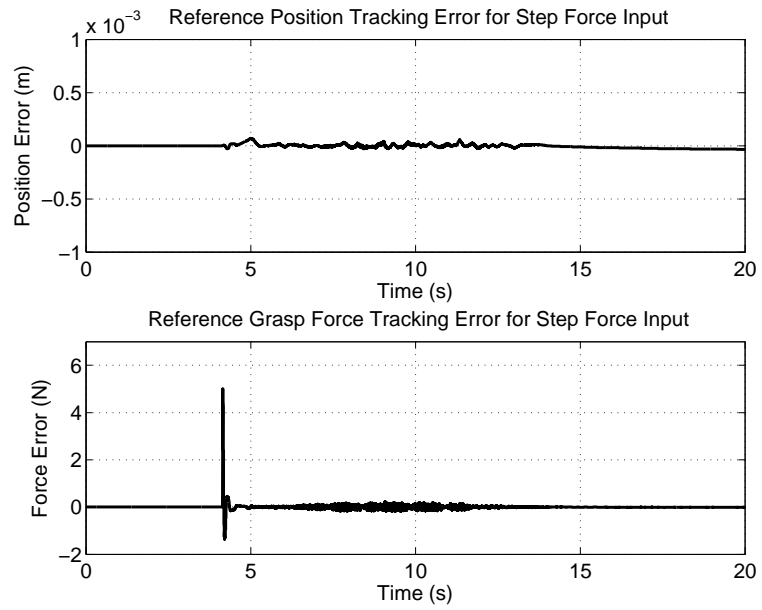


Figure 2.11: Position and force error for step force input

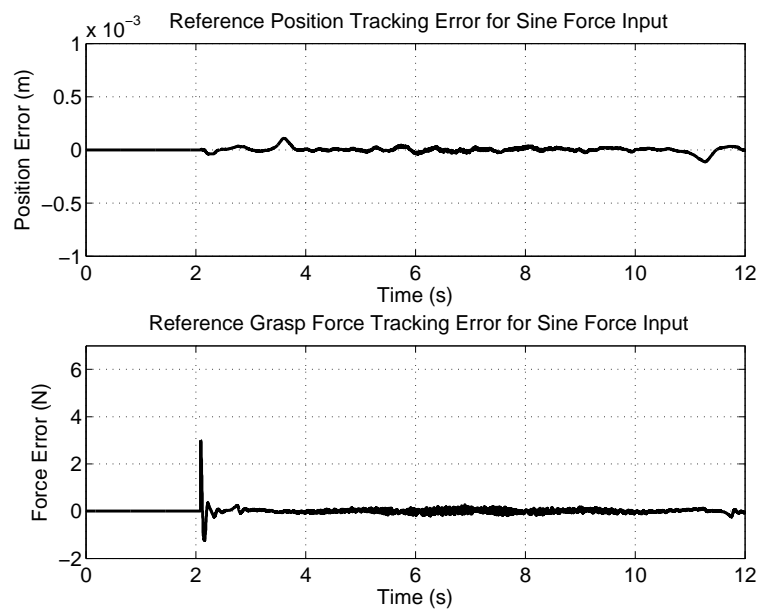


Figure 2.12: Position and force error for sine force input

## 2.4 Performance Improvement

In order to improve the overall system performance, one needs better observers that can give fast, accurate and smooth results. In order to meet this necessity, in this section, a new functional observer that can be used to estimate the velocity, acceleration and disturbance response of a motion control system is constructed. The objectives of the observer are both to achieve estimation that is as accurate as possible and to provide bandwidth that is as large as possible. The functional structure of the observer enables it to be used for the estimation of velocity, acceleration or disturbance with some changes in the observer parameters.

### 2.4.1 System Description

The depiction of a classical motion control system is given in Figure 2.13. Here,  $I^{ref}(s)$  and  $T_{dis}(s)$  stand for the Laplace Transformed current input

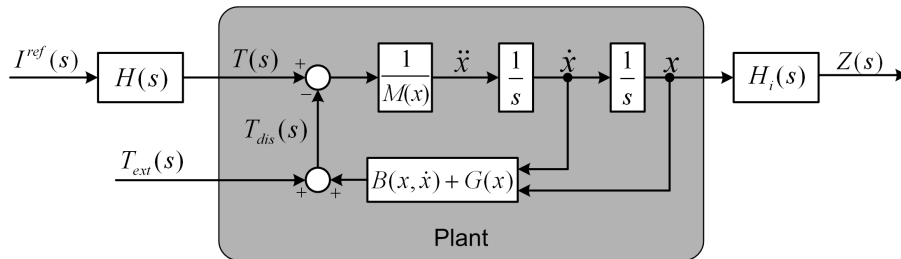


Figure 2.13: Structure of a motion control system with ideal observer

and disturbance acting on the system respectively. As mentioned earlier, the feedback terms  $B(x, \dot{x})$  and  $G(x)$  represent the viscous friction and gravity acting on the system respectively. In this general system, the input current

to the system can be transferred through a transfer function;

$$T(s) = H(s)I^{ref}(s)$$

where  $T(s)$  is the input torque. Without loss of generality, one can lump the non-idealities in the input torque formulation to the disturbance term and come up with a constant gain. This way the system input becomes,

$$T(s) = K_n I^{ref}(s) \quad (39)$$

with  $K_n$  being the nominal torque constant that maps the input current to the input torque. The response of a second order plant can be represented by,

$$R(s) = \frac{1}{M(x)s^2} \quad (40)$$

where,  $x$  is the generalized coordinate of motion and  $M(x)$  stands for the plant inertia. Considering the disturbance as an additional input to the system, the output of the structure given in Figure 2.13 can be written as;

$$X(s) = R(s) \{H(s)I^{ref}(s) - T_{dis}(s)\} \quad (41)$$

where,  $R^{-1}(s) = M_n s^2$  with  $M_n$  representing the nominal inertia of the system.

In order to acquire measurements of the system, one has to incorporate the plant output,  $X(s)$  with a transfer function. In the structure shown in Figure 2.13,  $Z(s)$  is the variable of interest that is related to the plant output by the ideal (not necessarily realizable) transfer function  $H_i(s)$  (i.e;  $Z(s) = H_i(s)X(s)$ ). If output  $Z(s)$  cannot be directly measured, then  $H_i(s)$  stands

for the ideal transfer function of the observer that needs to be designed. However, the content of this observer may not be physically realizable if  $H_i(s)$  is an improper transfer function like  $\eta_1 s^2 + \eta_2 s + \eta_3$  (i.e. a linear combination of acceleration, velocity and position). For such cases, one can utilize an approximate structure as shown in Figure 2.14 and come up with an estimate of the output  $Z(s)$ . In this second structure, assuming that the disturbance term is transferred to the estimation by transfer function  $H_d(s)$ , one can write the error due to unmeasured inputs as

$$\Delta Z(s) = H_d(s) T_{dis}(s) \quad (42)$$

In designing the observer, the main criteria is to select the error in the estimated variable  $\hat{Z}(s)$  to have a desired value of zero.

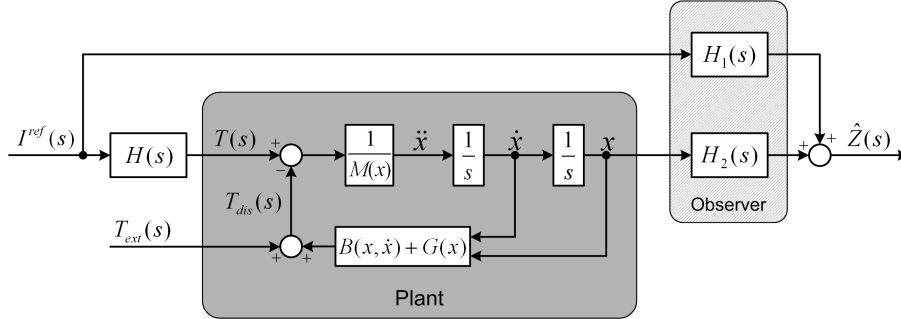


Figure 2.14: Proposed observer structure

Now the problem can be formulated as follows: For the system given in Figure 2.14, using the nominal plant parameters and measurable outputs (i.e.  $I^{ref}(s)$  and  $X(s)$ ), find transfer functions  $H_1(s)$  and  $H_2(s)$  that will best approximate the variable of interest  $Z(s)$ .

### 2.4.2 Observer Construction

Using equations (39), (40), (41) and the structures shown in Figure 2.13 and Figure 2.14, one can write the actual and the estimated values of  $z$  as follows:

$$\begin{aligned} Z(s) &= H_i(s)X(s) + H_d(s)T_{dis}(s) \\ Z(s) &= H_i(s)R(s) \{H(s)I^{ref}(s) - T_{dis}(s)\} + H_d(s)T_{dis}(s) \end{aligned} \quad (43)$$

$$\begin{aligned} \hat{Z}(s) &= H_2(s)X(s) + H_1(s)I^{ref}(s) \\ \hat{Z}(s) &= H_2(s)R(s) \{H(s)I^{ref}(s) - T_{dis}(s)\} + H_1(s)I^{ref}(s) \end{aligned} \quad (44)$$

From (43) and (44), one can write the error in the estimation as follows:

$$\begin{aligned} \Delta Z(s) = Z(s) - \hat{Z}(s) &= \{R(s)H(s)(H_i(s) - H_2(s)) - H_1(s)\} I^{ref}(s) \\ &\quad - \{R(s)(H_i(s) - H_2(s)) - H_d(s)\} T_{dis}(s) \end{aligned} \quad (45)$$

The difference between desired output  $Z(s)$  and its estimated value  $\hat{Z}(s)$ , as expressed in (45) depends on both control input and the disturbance. In order to push this estimation error to zero, coefficients of both current ( $I^{ref}(s)$ ) and disturbance ( $T_{dis}(s)$ ) should be imposed to have zero value. Letting those coefficients be equal to zero and solving further, one finds the following two equations for the transfer functions  $H_1(s)$  and  $H_2(s)$ ;

$$\begin{aligned} H_1(s) &= H(s)H_d(s) \\ H_2(s) &= H_i(s) - R^{-1}(s)H_d(s) \end{aligned} \quad (46)$$

The implicit assumption made in (39) saying that the torque can be transmitted to the plant with a constant gain (i.e.  $H(s) = K_n$ ) results in  $H_1(s)$  being equal to a scalar multiple of  $H_d(s)$ . This result is very important since it implies that the error due to disturbance is compensated by the current input during estimation. In other words, the observer, while using position information and transfer function  $H_2(s)$  to acquire the estimated value, also uses the current information and transfer function  $H_1(s)$  along with the nominal parameters of the plant to cancel the effect of disturbance in estimation.

In order to solve for  $H_1(s)$  and  $H_2(s)$  we can define a generalized transfer function for  $H_d(s)$ . Since the disturbance acting on the system pass through a second order dynamics, we can formulate this generalized transfer function as follows;

$$H_d(s) = \frac{g^2 s(\gamma s + \delta)}{M_n (s + g)^2} \quad (47)$$

where,  $M_n$  represents the nominal inertia of the plant. Using this error, the expression for  $R$  from (40) and equation (46), generalized forms for the transfer functions  $H_1(s)$  and  $H_2(s)$  can also be defined;

$$H_1(s) = \frac{K_n g^2 s(\gamma s + \delta)}{M_n (s + g)^2} \quad (48)$$

$$H_2(s) = H_i(s) - \frac{g^2 s^3(\gamma s + \delta)}{(s + g)^2} \quad (49)$$

In both of the equations (48) and (49), the coefficients  $g$ ,  $\gamma$  and  $\delta$  should be selected in design process. In order to design the parameters, we have to refer to the format of the ideal transfer function  $H_i(s)$ . Let the ideal transfer function be  $H_i(s) = \alpha s^2 + \beta s$ ; in other words let us assume that a linear combination of velocity and acceleration is to be estimated. Substituting



$H_i(s)$  into (49), one can obtain;

$$H_2(s) = (\alpha s^2 + \beta s) - \frac{g^2 s^3 (\gamma s + \delta)}{(s + g)^2}$$

which can be expanded further as follows,

$$H_2(s) = \frac{C_4 s^4 + C_3 s^3 + C_2 s^2 + C_1 s}{(s + g)^2} \quad (50)$$

where,

$$\begin{aligned} C_4 &= \alpha - g^2 \gamma \\ C_3 &= 2g\alpha - g^2 \delta + \beta \\ C_2 &= 2g\beta + g^2 \alpha \\ C_1 &= g^2 \beta \end{aligned}$$

Since, for a physical system, the estimator will have at most second degree derivative, we can set the coefficients of  $s^4$  and  $s^3$  terms ( $C_4$  and  $C_3$ ) be equal to zero, which gives;

$$\begin{aligned} \alpha - g^2 \gamma &= 0 \\ \gamma &= \frac{\alpha}{g^2} \end{aligned} \quad (51)$$

$$\begin{aligned} 2g\alpha - g^2 \delta + \beta &= 0 \\ \delta &= \frac{\beta + 2g\alpha}{g^2} \end{aligned} \quad (52)$$

Substituting (51) and (52) into (48) and (49) gives the following set of transfer

functions:

$$\begin{aligned}
 H_1(s) &= \frac{K_n \alpha s^2 + (\beta + 2g\alpha)s}{M_n (s + g)^2} \\
 H_2(s) &= gs \frac{(g\alpha + 2\beta)s + g\beta}{(s + g)^2} \\
 H_i(s) &= \alpha s^2 + \beta s
 \end{aligned} \tag{53}$$

Now, the only design parameters are  $\alpha$  and  $\beta$  which is determined from the structure of the ideal observer  $H_i(s)$ . The functional observer can be realized using just two first order filters as depicted in Figure 2.15. This structure

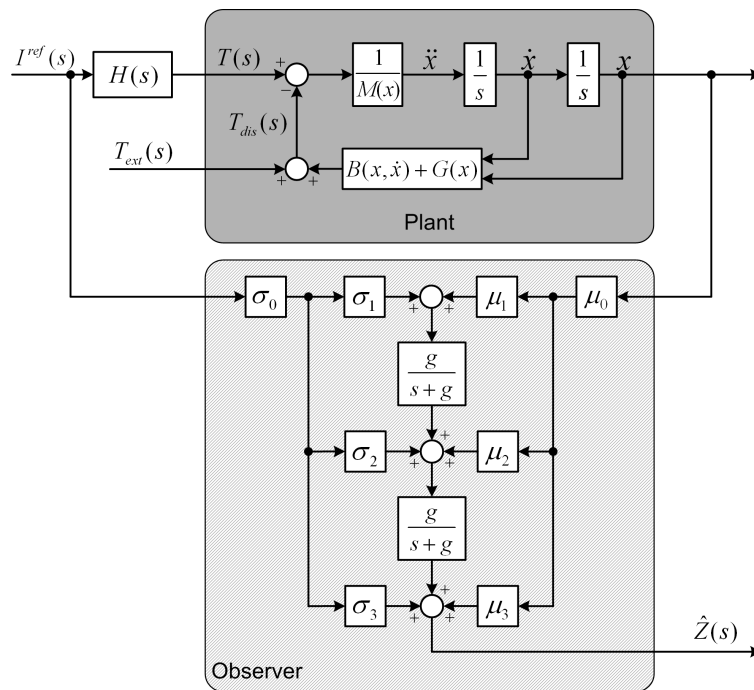


Figure 2.15: Block diagram of functional observer

mathematically imposes the following two equations.

$$H_1(s) = \frac{\alpha s^2 + (\beta + 2g\alpha)s}{M_n(s+g)^2} = \sigma_0 \left( \sigma_3 + \frac{\sigma_2 g}{(s+g)} + \frac{\sigma_1 g^2}{(s+g)^2} \right) \quad (54)$$

$$H_2(s) = \frac{(g^2\alpha + 2g\beta)s^2 + g^2\beta s}{(s+g)^2} = \mu_0 \left( \mu_3 + \frac{\mu_2 g}{(s+g)} + \frac{\mu_1 g^2}{(s+g)^2} \right) \quad (55)$$

The values for gains  $\sigma_i$  and  $\mu_i$  ( $i = 0, 1, 2, 3$ ) can be found by substituting the necessary numbers for  $\alpha$  and  $\beta$  to the ideal observer  $H_i(s)$ . A summary of the coefficients for velocity, acceleration and disturbance estimation is given in Table 2.3

Table 2.3: Parameters of the Functional Observer for Different Configurations

$H_i$	$0s^2 + s$	$s^2 + 0s$	$K_n \dot{t}^{ref} - M_n s^2$
$(\hat{z})$	$(\dot{x})$	$(\ddot{x})$	$(\tau_{dis})$
-----	-----	-----	-----
$\sigma_0$	$\frac{K_n}{gM_n}$	$\frac{K_n}{M_n}$	$-K_n$
$\sigma_1$	$-1$	$-1$	$-1$
$\sigma_2$	$1$	$0$	$0$
$\sigma_3$	$0$	$1$	$0$
$\mu_0$	$g$	$g^2$	$-M_n g^2$
$\mu_1$	$1$	$1$	$1$
$\mu_2$	$-3$	$-2$	$-2$
$\mu_3$	$2$	$1$	$1$

### 2.4.3 Experimental Results

The proposed observer is tested using one of the two identical linear motors. In order to validate the velocity estimation, two different experiments are handled. In the first experiment, constant velocity references were given to the system and in the second experiment, a trapezoidal velocity profile is given to the system. In order to explicitly indicate the improvement, the output of the proposed structure is compared to a first order filtered derivative which is also referred as the classical observer. Results of the velocity experiments are given in Figure 2.16 and Figure 2.17. As it is clear from the graphs, the proposed structure performs much better than the first order filtered derivative.

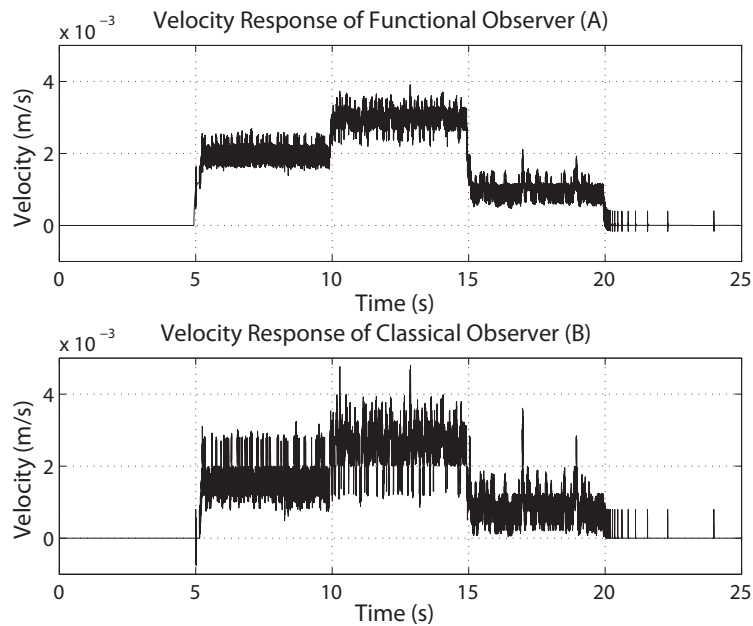


Figure 2.16: Velocity responses for step velocity reference

For the depiction of acceleration estimation performance, the system is operated under two consecutive pulse inputs of different signs and the results

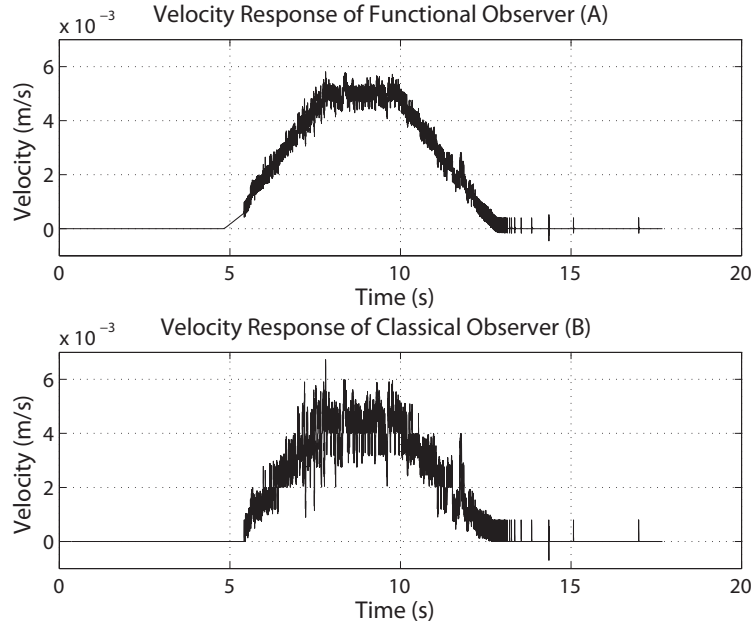


Figure 2.17: Velocity responses for trapezoidal velocity reference

are given in Figure 2.18. In this figure, the red curve shows the output of a second order double filtered differentiator and the blue curve shows the output of the proposed estimator. For the acceleration experiment, in order to have a better comparison, the position response of the encoder is saved and double differentiated offline using a window size of 5 consecutive steps and this result is also shown in Figure 2.18 (black curve). From the graphs, it is obvious that the estimator performance is much closer to the actual response.

Finally, the disturbance estimation result are also validated experimentally. Figure 2.19 shows the estimation result obtained from the proposed observer and the result of classical well known disturbance observer. Clearly, the proposed structure gives smoother results for the disturbance estimation. However, since the proposed scheme includes two filters while classical DOB

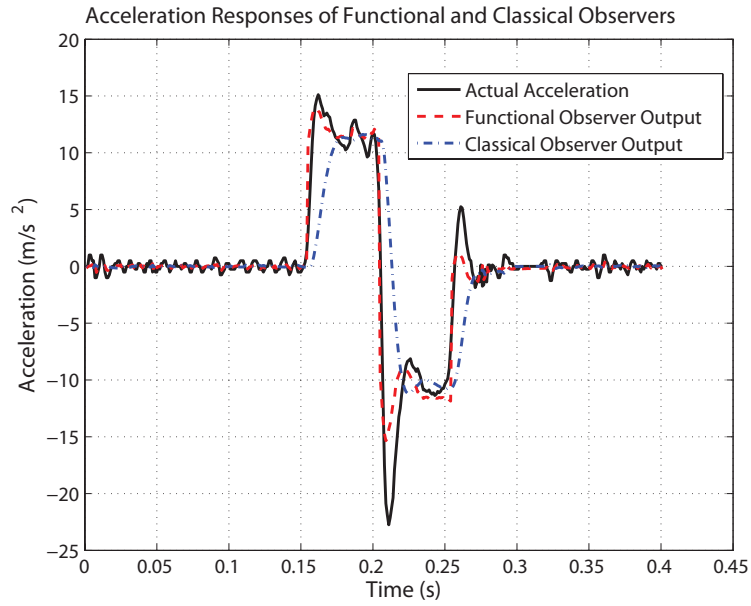


Figure 2.18: Acceleration responses

has only one filter, it cannot perform as fast as classical DOB. It should be noted here that, since fast rejection of the disturbance is of crucial importance, classical DOB is advised to be used instead of the disturbance estimation obtained from the proposed observer.

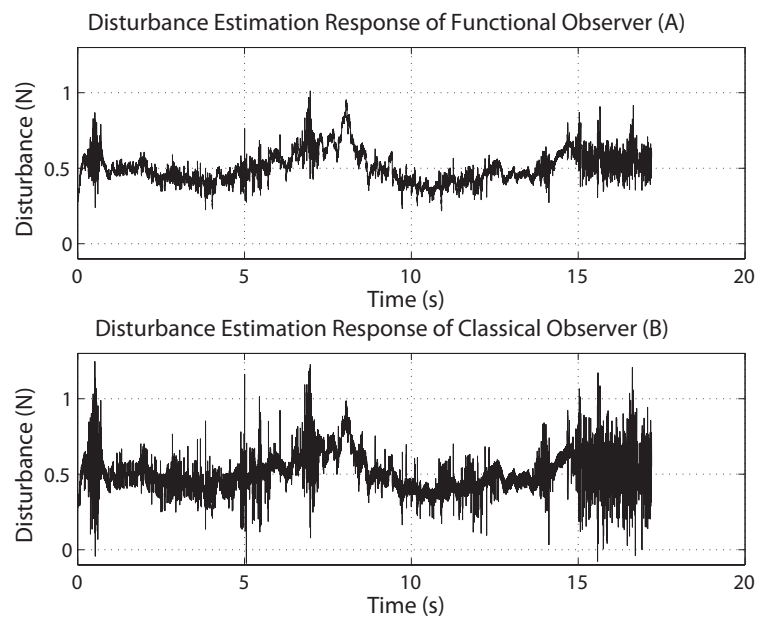


Figure 2.19: Disturbance estimation responses

# Chapter III

## 3 Bilateral Control with Time Delay

In this chapter, bilateral teleoperation with time delays is considered. As mentioned earlier, the medium for teleoperation is consisted of network (usually internet environment) that can exhibit time delay in data transmissions. A schematic drawing of a motion control system with and without time delay is given in Figure3.1 below.

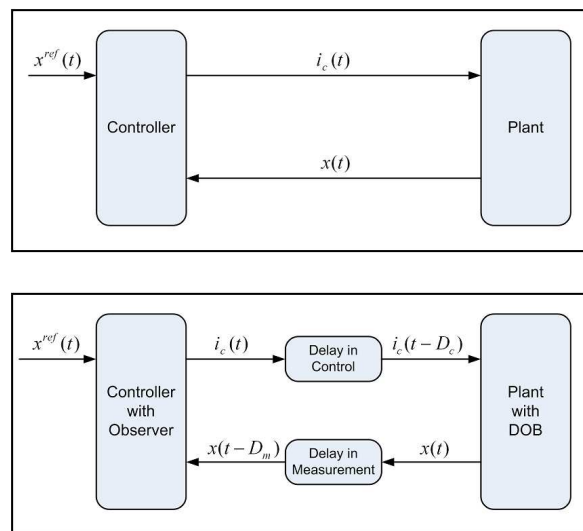


Figure 3.1: Representative drawing of normal and delayed system

Due to the structure of network, both the measurements from the remote



plant and the control input to the remote side arrives with unknown time delays. Under these conditions, the goal of a controller for time delayed bilateral teleoperation should be providing stable operation with as much transparency as possible.

### 3.1 Position Control Under Time Delay

In order to have stable position tracking under time delay, it is necessary to have an observer that can overcome the measurement delay from the slave side and can give on time estimation of the slave motion. The master side controller can then make use of this estimator output to create the necessary control input for position tracking. The following analysis includes the implementation of a previously proposed network control structure [42]. For that purposed, derivation of this previously proposed structure is made in a slightly different way. Moreover, all of the analysis is made over a one DOF motion control system. Without loss of generality, the results obtained from this structure can then be applied to MIMO systems. For the controller design, it is assumed that nominal parameters of the plant are known and the measurements are subject to network non ideality (delay and dynamic distortions) while the control input is subject only to network delay.

#### 3.1.1 Problem Definition

Let us assume that a one DOF motion control system is to be manipulated over a network that contains unknown time delay both in measurement and control channels. Due to the nature of delay, both control input and measurements from the plant will be nonlinearly distorted. The plant dynamics for such a system was given in (10) and (11) and can be summarized as

$$M_n \ddot{x}(t) = K_n i_c(t) - \tau_{dis}(t)$$

where,  $\tau_{dis}(t)$ ,  $K_n$  and  $M_n$  stand for the total disturbance torque acting on the plant, nominal torque constant and nominal plant inertia respectively.

Assuming position and velocity of the slave plant is available at the remote location, when there is delay  $D_m$  in the measurement channel, controller can only access the delayed position and velocity (i.e.  $x(t - D_m)$  and  $\dot{x}(t - D_m)$ ). So, it is necessary to use an observer that can give the predictions of the remote plant position and velocity synchronized with the actual outputs, that is without any delays. In that sense, one can define that the goal is to design observer based on available measurements  $x(t - D_m)$ ,  $\dot{x}(t - D_m)$  and control input  $K_n i_c$  with zero estimation error. Once the actual output of the slave plant is estimated, then this can be used in another controller to generate the input to the remote plant.

### 3.1.2 Observer and Controller Construction

Under the assumption that slave plant has nominal behavior with integrated DOB and perceiving the total effect of measurement delay as a network disturbance acting on the estimator, one can introduce a second observer over the network to come up with an initial estimate of the slave plant velocity. Using the available data, the total network disturbance can be given as follows

$$\tau_{dis}^{nw}(t) = K_n i_c(t) - M_n \ddot{x}(t - D_m) \quad (56)$$

Just like the conventional disturbance observer structure, the estimation of this network disturbance can be made using delayed slave plant velocity and a low pass filter. The estimated network disturbance stand for the torque that is supposed to act on the slave plant during measurement delay. Since the slave plant is enforced to behave nominal with DOB, the estimated network disturbance can be passed through the nominal inertia of slave plant and be

integrated to give the velocity difference that is supposed to exist during the delay time. In mathematical terms, this can be expressed as

$$\Delta\dot{x}(t) = \int \frac{1}{M_n} \tau_{dis}^{nv}(\xi) d\xi \quad (57)$$

Addition of this velocity difference to the delayed velocity gives the estimated velocity of the slave plant as shown below:

$$\hat{\dot{x}}(t) = x(t - D_m) + \Delta\dot{x}(t) \quad (58)$$

Under the assumption that initial conditions of the slave system and the observer output are the same and perfect disturbance cancelation is available, this observer can track the slave velocity without any delay. However, there is no guarantee about the initial conditions being equal and perfect disturbance rejection is not always feasible. So, one has to insert additional compensation to push the estimated states (i.e. position and velocity) to the actual slave plant output. So, including the position and velocity the estimation error can be written in the following general format:

$$e_{\hat{x}}(t) = C_1(x(t) - \hat{x}(t)) + C_2(\dot{x}(t) - \hat{\dot{x}}(t)) \quad (59)$$

In order to enforce an exponential convergence of error to zero, one can impose the following error dynamics on the system:

$$\dot{e}_{\hat{x}}(t) + K_x e_{\hat{x}}(t) = 0 \quad (60)$$

Substituting the error given in (59) into (60), and collecting the actual and estimated parameters together, the following condition for the observer and estimator can be obtained:

$$\begin{aligned} & \{C_2\ddot{x}(t) + (K_x C_2 + C_1)\dot{x}(t) + K_x C_1 x(t)\} \\ - & \{C_2\hat{\hat{x}}(t) + (K_x C_2 + C_1)\hat{\hat{x}}(t) + K_x C_1 \hat{x}(t)\} = 0 \end{aligned} \quad (61)$$

Equation (61) can be satisfied when both of the terms inside the curly brackets are independently equal to zero. Solving these equations results in following convergence accelerations be inserted to the estimator and slave plant respectively:

$$\begin{aligned} \ddot{x}_{con}(t) &= -\frac{(K_x C_2 + C_1)}{C_2} \dot{x}(t) - \frac{K_x C_1}{C_2} x(t) \\ \hat{\hat{x}}_{con}(t) &= -\frac{(K_x C_2 + C_1)}{C_2} \hat{\hat{x}}(t) - \frac{K_x C_1}{C_2} \hat{x}(t) \end{aligned} \quad (62)$$

Having in mind that the acceleration reference can be converted to the current reference by a scaler, one can finally summarize the expression given in equation (62) as follows:

$$\begin{aligned} i_{con}(t) &= -K_D \dot{x}(t) - K_P x(t) \\ \hat{i}_{con}(t) &= -K_D \hat{\hat{x}}(t) - K_P \hat{x}(t) \end{aligned} \quad (63)$$

where the content of convergence parameters  $K_P$  and  $K_D$  are given in Table 3.1.2

With the addition of convergence terms both to the estimator and the slave plant, it is now guaranteed that the estimation of the remote plant

$K_P$	$K_D$
-----	-----
$\frac{M_n K_x C_1}{K_n C_2}$	$\frac{M_n (K_x C_2 + C_1)}{K_n C_2}$

Table 3.1: Parameters of the Time Delayed Position Controller

response is synchronized on time with that of the actual slave output. Now the only remaining thing is to construct a controller to generate the control current which may then be sent to the slave system after a control channel delay  $D_c$ . Assuming the position and velocity commands from the master side is available to the controller, the controller error can be defined as:

$$e_c = C_1(x_m(t) - \hat{x}_s(t)) + C_2(\dot{x}_m(t) - \dot{\hat{x}}_s(t)) \quad (64)$$

Utilizing a PD controller for the tracking of master position reference leads the following control current be used as the control input to both the slave system and the observer:

$$i_c(t) = K_P^{con}(x_m(t) - \hat{x}_s(t)) + K_D^{con}(\dot{x}_m(t) - \dot{\hat{x}}_s(t)) \quad (65)$$

Now, the entire observer-controller structure for the position control under time delay is obtained. A block diagram of the above-derived structure is depicted in Figure 3.2 below. In order to analyze the stability of this scheme, the total controller output that the slave system receives can be investigated. With the addition of convergence term, the slave plant receives the following

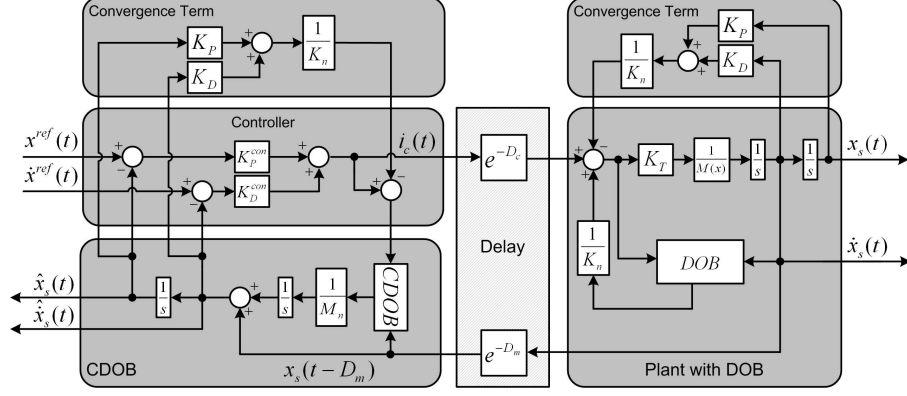


Figure 3.2: Representative drawing network controller

input acceleration

$$\begin{aligned} \ddot{x}_s^{ref}(t) = & -K_P x_s(t) - K_D \dot{x}_s(t) + K_P^{con} x_m(t - D_c) - K_P^{con} \hat{x}_s(t - D_c) \\ & + K_D^{con} \dot{x}_m(t - D_c) - K_D^{con} \hat{x}_s(t - D_c) \end{aligned} \quad (66)$$

In equation (66), since the terms  $K_P^{con} x_m(t - D_c)$  and  $K_D^{con} \dot{x}_m(t - D_c)$  are the references to the controller, when talking about closed loop stability, they can be disregarded. The remaining part of (66) can be rearranged and written in the following state space format:

$$\begin{bmatrix} \dot{x}_s \\ \ddot{x}_s \end{bmatrix} = \begin{bmatrix} 0 & 1 \\ -K_P & -K_D \end{bmatrix} \begin{bmatrix} x_s \\ \dot{x}_s \end{bmatrix} + \begin{bmatrix} 0 & 0 \\ -K_P^{con} & -K_D^{con} \end{bmatrix} \begin{bmatrix} x_s(t - D_c) \\ \dot{x}_s(t - D_c) \end{bmatrix}$$

Once the closed loop system is expressed in this format, stability analysis can be made in terms of matrices. In [69] it is shown that for systems represented in the following form

$$\dot{\mathbf{x}}(t) = \mathbf{A}_1 \mathbf{x}(t) + \mathbf{A}_2 \mathbf{x}(t - \tau) \quad (67)$$

the stability requires  $\mathbf{A}_1 + \mathbf{A}_2$  to be Hurwitz, and that there exists positive definite symmetric matrices  $\mathbf{P}, \mathbf{S}, \mathbf{R}$  such that

$$\mathbf{A}_1^T \mathbf{P} + \mathbf{P} \mathbf{A}_1 + \mathbf{P} \mathbf{A}_2 \mathbf{S}^{-1} \mathbf{A}_2^T \mathbf{P} + \mathbf{S} + \mathbf{R} = \mathbf{0} \quad (68)$$

Due to the fact that matrices  $\mathbf{A}_1$  and  $\mathbf{A}_2$  depend on the design parameters (the observer convergence gains and the controller gains) and not on the plant parameters, one may use this stability conditions to determine range of the design parameters for which stability for the closed loop system will be ensured for selected matrices  $\mathbf{P}, \mathbf{S}, \mathbf{R}$ .

### 3.1.3 Experimental Results

The network position controller explained in the previous section is implemented on the experimental platform described before. The experiments are conducted with time delay in both measurement and control channels. To approximate the most realistic scenario, the structure of the time delay is adjusted to have variation within a certain range over a constant value. During the first set of experiments, one of the identical motors (the master system) were controlled under computer generated step and sine references while the position and velocity readout of this system were sent as input to the second motor (the slave system). Figure 3.3 and Figure 3.4 depicts the first set of experiments for which a variable delay of 20 ms was added on top of a 500 ms constant delay both in measurement and control channels.

The controller gains for the given experiments were tuned to be  $K_P^{con} = 980$  and  $K_D^{con} = 2.1$  while the convergence gains were set to have the values  $K_P = 25$  and  $K_D = 8$ . The filter in DOB is set to the value  $g = 1000$  while



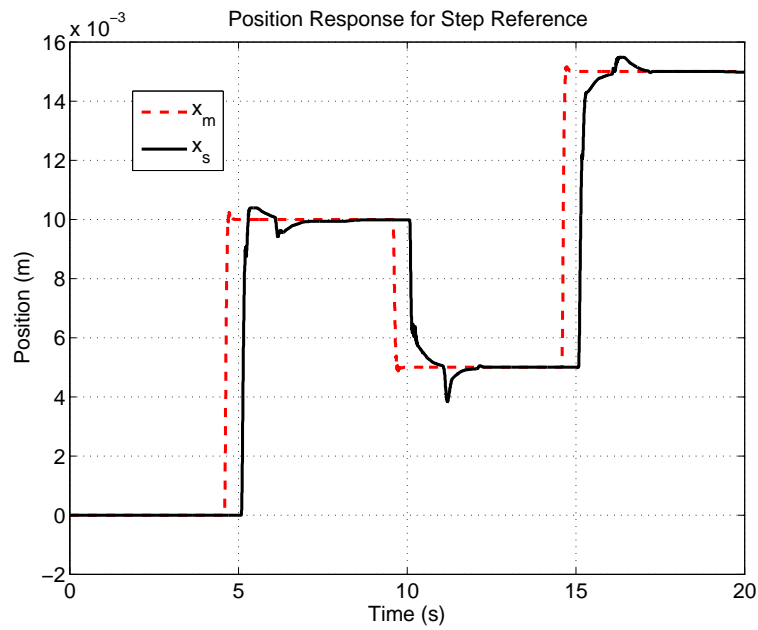


Figure 3.3: Position response for step reference

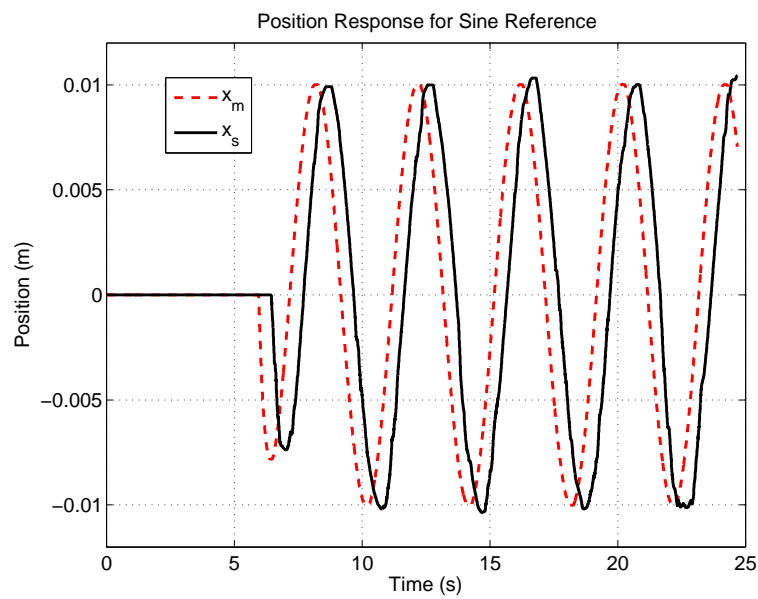


Figure 3.4: Position response for sine reference

the filter in velocity has the value  $g = 200$ . In the second set of experiments, the input to the slave system was again created from the position and velocity measurement of the master system. However, in this second set, the input to the master system was not a computer generated reference. Instead, a human operator moved the master system with an arbitrary motion to see the closed loop behavior of the proposed controller under random references. The result of random motion experiment, depicted in Figure 3.5 indicates a further realization of motion synchronization for master slave teleoperation systems operated under arbitrary network delay. The stability of the slave system was preserved during motion while a very satisfactory tracking is achieved. In the second set, experiments were conducted for a variable time delay of 50 ms added to a constant delay of 500 ms both in measurement and control channels.

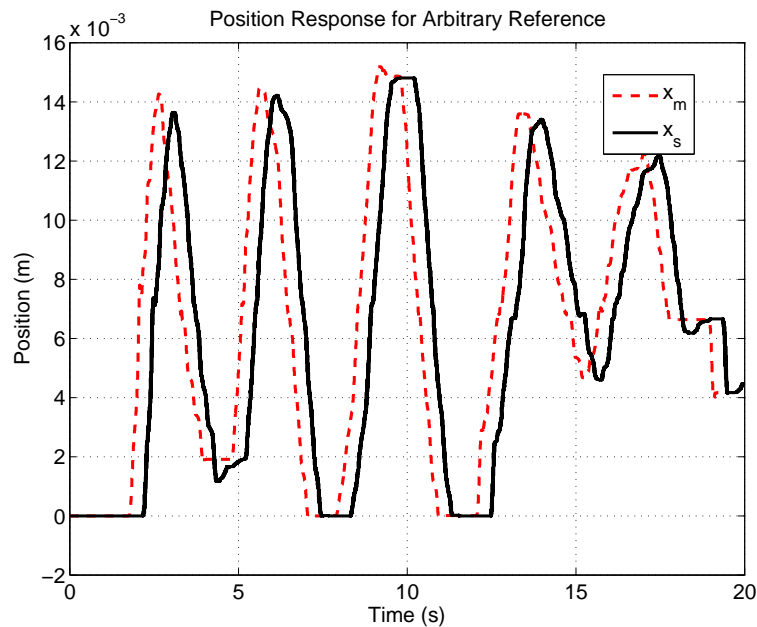


Figure 3.5: Position response for arbitrary reference

### 3.1.4 Additional Compensation for Environment Contact

In the previous section, it is shown that in free motion tracking, the network observer is performing very well. In this structure it is assumed that the slave plant is enforced to behave nominal with DOB. However, it was previously shown in (14) that due to the low pass filter used in the structure of DOB, the actual system is always subject to non-idealities and perfect rejection of disturbance might not always be possible. In this section, the imperfection in disturbance rejection is analyzed mathematically and additional compensation structure is proposed to push the slave plant to perfectly nominal structure. Since the disturbance estimation in DOB is made via a low pass filter, one can write down the total estimation error in DOB as follows:

$$\begin{aligned}
 \delta\tau_{dis} &= \tau_{dis} - \hat{\tau}_{dis} \\
 \delta\tau_{dis} &= \tau_{dis} - \tau_{dis} \left( \frac{g_d}{s + g_d} \right) \\
 \delta\tau_{dis} &= \tau_{dis} s \frac{1}{g_d} \left( \frac{g_d}{s + g_d} \right)
 \end{aligned} \tag{69}$$

As obvious from (69), the remaining disturbance estimation error in classical DOB scheme includes the filtered and scaled derivative of the disturbance acting on the system. Since it is impossible to have an infinite filter gain  $g_d$ , there is always an error proportional to the derivative of the total disturbance. Because of this, in cases where disturbance torque changes very fast and with a uniform sign (i.e. either increase or decrease), the total error in disturbance rejection becomes effective. The environment contact forces, unlike the other disturbances acting on the plant, has such a structure. An experimental verification of this phenomena is given in Figure 3.6 in which the master

reference is sent to the slave plant after a time delay and both ideal reference and the actual responses are plotted. As it is obvious from the figure, the tracking error is proportional to the speed of motion (i.e. rate of change of disturbance).

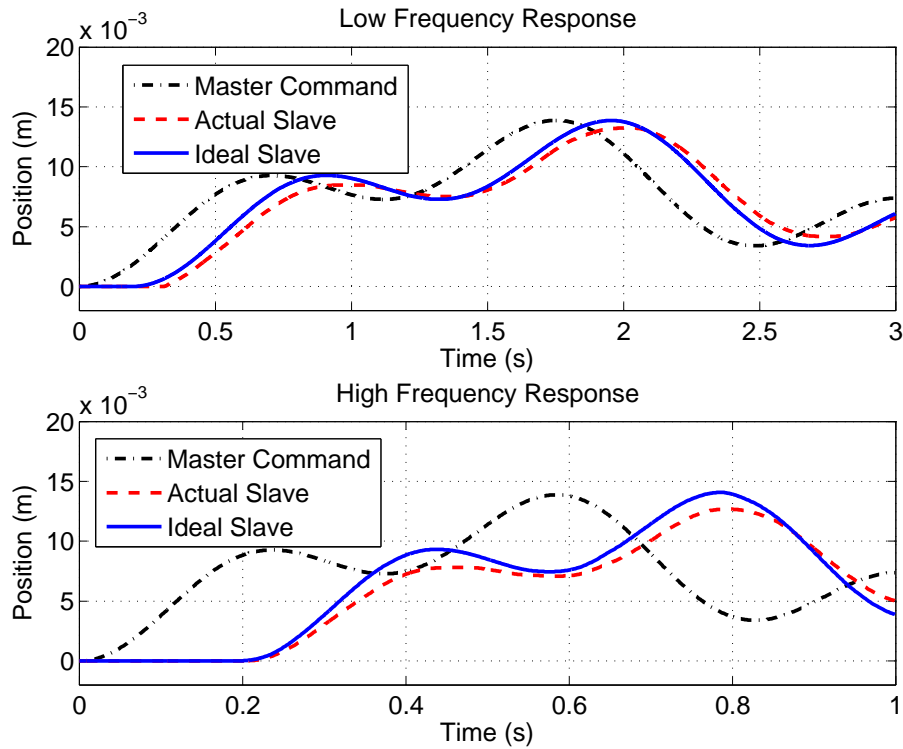


Figure 3.6: Tracking error in contact motion

For the problem described above, a model following control scheme is proposed. The structure of the controller is based on the use of a virtual slave plant model that is identical to the actual slave system except the fact that it does not include any environment model. In this structure, since the virtual model is fed with the same input to the slave plant and since it does not involve the effect of environment on total disturbance, it can generate the ideal trajectory for the slave plant motion. Once this ideal reference

is generated, additional compensation can be inserted to the actual slave plant using the error between actual slave and virtual slave model. For the generation of additional compensation, a discrete time sliding mode controller (SMC) is used. The block diagram of the model following controller is given in Figure 3.7 below. Once the structure of the controller is described, one

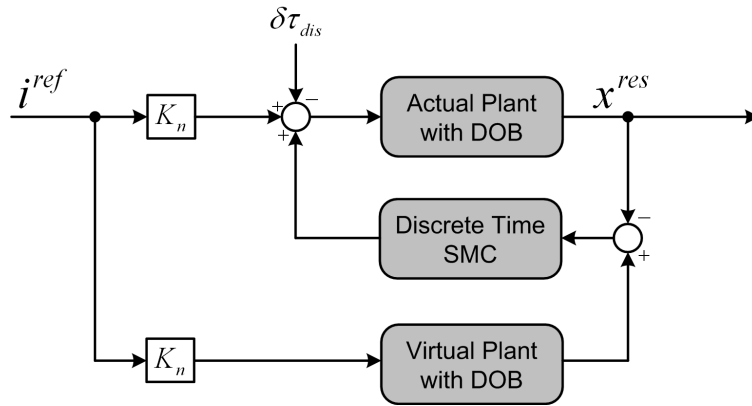


Figure 3.7: Model following controller structure

can continue with the derivation of the discrete time SMC controller.

The error between virtual and actual plants can be represented in the following vector form:

$$\xi = \begin{bmatrix} \Delta x \\ \Delta \vartheta \end{bmatrix} \doteq \begin{bmatrix} x^{vir} - x^{act} \\ \vartheta^{vir} - \vartheta^{act} \end{bmatrix} \quad (70)$$

where, the superscripts "vir" and "act" represent the virtual and actual plant outputs respectively. For sliding mode design, one can pick the following manifold to enforce a zero rate of change for a general linear combination of

the position and velocity errors;

$$\sigma = G\xi = \begin{bmatrix} \alpha & \beta \end{bmatrix} \begin{bmatrix} \Delta x \\ \Delta \vartheta \end{bmatrix} \quad (71)$$

with  $G \in \mathbb{R}^{1 \times 2}$ . For this system, in order to enforce finite time convergence, the following dynamics can be written on  $\sigma$

$$\dot{\sigma} + \lambda\sigma + \mu \cdot \text{sign}(\sigma) = 0 \quad (72)$$

where  $\lambda$  is necessarily positive definite in order to satisfy the Lyapunov stability condition. From the definition of sliding mode, the derivative of the manifold can also be expressed in terms of the equivalent control as follows:

$$\dot{\sigma} = GB(u^{eq} - u) \quad (73)$$

Inserting (73) back to the imposed finite time converging dynamics (72), one can come up with the following equation:

$$GB(u^{eq} - u) + (\lambda\sigma + \mu \cdot \text{sign}(\sigma)) = 0 \quad (74)$$

Now, in light of equation (74) and keeping in mind that the implementation will be made on a discrete time system, one can finally write down the following recursion for the controller:

$$u[k] = u[k - 1] + (GB)^{-1}(\lambda\sigma + \mu \cdot \text{sign}(\sigma)) \quad (75)$$

For the system under scope, the matrices  $G$  and  $B$  can be given as:

$$\begin{aligned} G &= \begin{bmatrix} \alpha & \beta \end{bmatrix} \\ B &= \begin{bmatrix} 0 & \frac{K_n}{M_n} \end{bmatrix}^T \end{aligned}$$

Substituting these matrices and  $\sigma$  from (71) back to equation (75), the recursion can be put to the following final form

$$u[k] = u[k - 1] + \frac{M_n}{K_n} \left\{ \frac{\lambda}{\beta}(\alpha\Delta x + \beta\Delta\vartheta) + \frac{\mu}{\beta}(\text{sign}(\alpha\Delta x + \beta\Delta\vartheta)) \right\} \quad (76)$$

### 3.1.5 Experimental Results

The developed model following controller scheme is tested on the experiments. In order to put more emphasis on position error, the error cost was selected as  $\begin{bmatrix} \alpha & \beta \end{bmatrix} = \begin{bmatrix} 5 & 1 \end{bmatrix}$ . Moreover, in order to reduce the chattering effect, the signum function coefficient was selected to be very small (i.e.  $\mu = 0.001$ ). And finally, exponential convergence rate was selected to be  $\lambda = 10$ .

During implementation, again a computer generated reference trajectory is used. After the addition of the proposed controller, it is observed that the slave system can exhibit perfect tracking of master reference after the control channel delay. The result of the experiment after additional compensation is depicted in Figure 3.8 and the errors corresponding to uncompensated and compensated structures are shown in Figure 3.9.

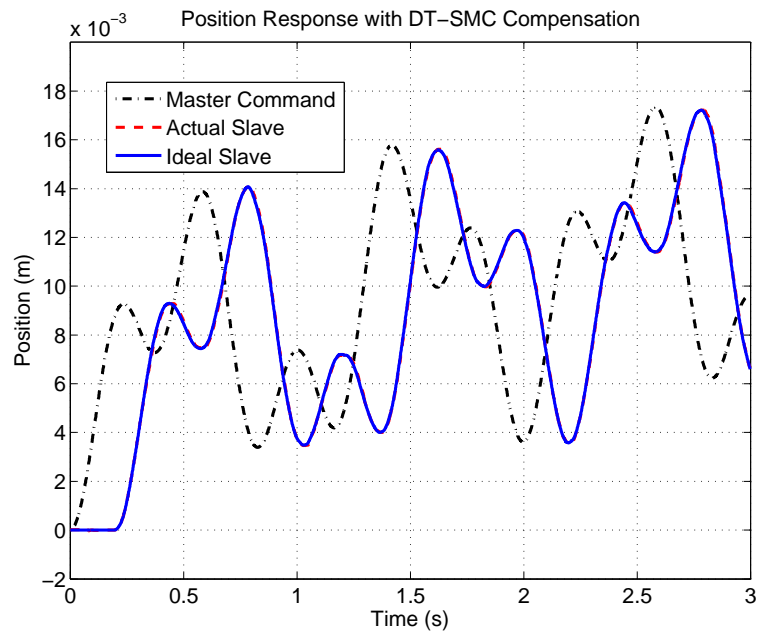


Figure 3.8: Environment contact motion with the proposed compensation

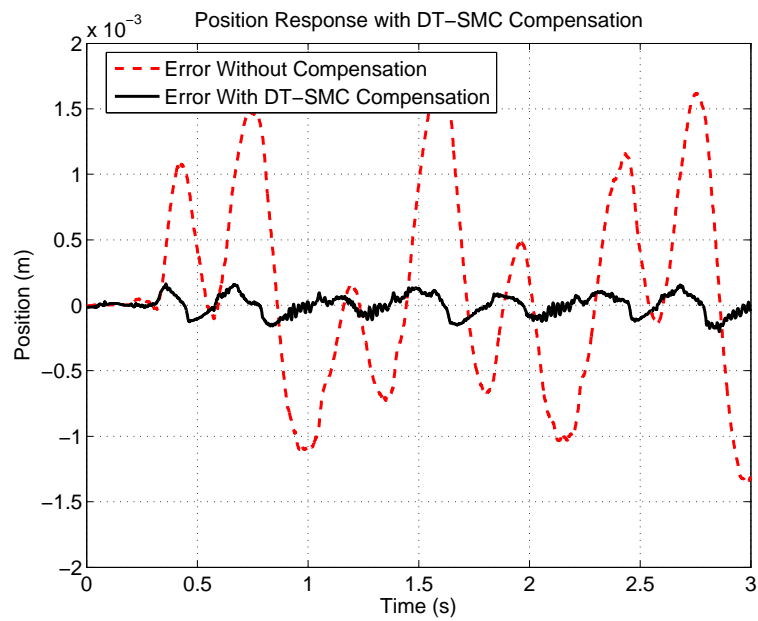


Figure 3.9: Compensated and uncompensated tracking errors



## 3.2 Force Control Under Time Delay

For the realization of actual bilateral control with time delay, on top of position control, the general structure of the controller should include the force control loop. However, force of the slave system arise due to its interaction with a remote environment. Since the measurement channel is subject to time delay, this force information can reach the master side after a time delay.

In this section, force control loop is added on top of the position control loop to obtain a bilateral teleoperation system with time delay. In that sense, first a straight forward implementation of local force control on the master side is made. In this first scheme, the controller used the force response of the slave system after the measurement delay. So, it is assumed that human operator is aware of the existence of delayed force feedback from the slave side.

Following the implementation of local controller, a new approach is proposed to utilize the force control. In this second approach, assuming that the environment location is a priori known by the master plant, the local force control is realized using the remote environment parameters. A force estimator is developed based on the remote environment parameters and a parameter adaptation law is realized that enables the convergence of the estimated stiffness to the actual one. Having in mind that the dominant portion of interaction forces arise due to the stiffness, it is assumed that the environment can be modeled as a linear spring. The novelty introduced with this method is the use of a relatively constant descriptor (i.e. environment stiffness) rather than a much more dynamic one (i.e. actual slave force). The proposed scheme enables the human operator feel the contact force before it

actually exists and hence improves the transparency in force control.

### 3.2.1 Local Force Controller

Compensation of delay in force measurement may not be realized using the same structure shown for position tracking. The reason is very simple; in estimation of position, known structure of the plant is used and there is no such nominal structure for the remote environment. Having this in mind, extension to bilateral control may establish full tracking in position since delay in position loop may be compensated with the estimation of slave plant motion. On the other hand, force tracking on the master side must be established as a separate local loop for which the slave force input is received after a delay. That would ask for reformulation of bilateral control problem as

$$e_x(t) = x_m(t) - \hat{x}_s(t) \quad (77)$$

$$e_F(t) = F_m(t) + F_s(t - D_m) \quad (78)$$

This structure is implemented in a local controller that has a similar structure to the one described in the previous chapter. The block diagram of the controller is depicted in Figure 3.10 and the experimental results are given in Figure 3.11 for position tracking and force tracking. Selection of control for position and force tracking should follow standard procedure of acceleration control method. In order to avoid loop with delay in force control on the slave side, the force control loop should be closed only on master side. Such a structure will guaranty stability.

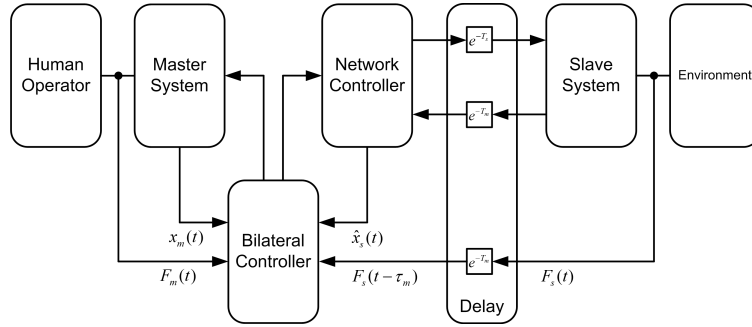


Figure 3.10: Block diagram of the local force controller

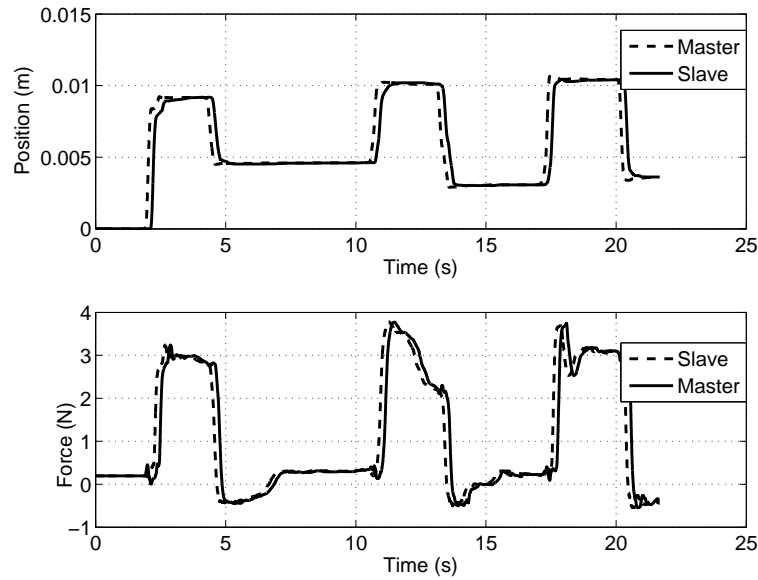


Figure 3.11: Experimental results of the local force controller

### 3.2.2 Estimated Force Control with Environment Adaptation

Although the local force controller that use the delayed slave force can provide stable operation, it is way beyond providing enough transparency for the operator. In order to reconstruct the slave force before the measurement delay, a new approach is utilized in this section. In the analysis below, a force estimator is developed based on a parameter adaptation law that

enables the convergence of the estimated stiffness to the actual one. It is assumed that the environment can be modeled as a linear spring with spring coefficient  $K_e$ . So, the estimate of forces due to the slave environment can be written in terms of estimated stiffness:

$$\hat{F}_s = \hat{K}_e x_e \quad (79)$$

where  $x_e$  is the deformation of the environment from the nominal position. In order to use the general indirect adaptive control scheme, one can write the following equation:

$$\tilde{F}_s = \tilde{K}_e x_e \quad (80)$$

where  $(\tilde{F}_s = F_s - \hat{F}_s)$  and  $(\tilde{K}_e = K_o - \hat{K}_e)$  with  $K_o$  being an initial estimate for the adaptation loop. Once this equation is defined, the adaptation law can be formulated using a Lyapunov technique by defining the following energy function;

$$V = \tilde{K}_e \alpha \tilde{K}_e \quad (81)$$

In order to have a negative definite derivative for this energy function, one can select the following parameter adaptation equation:

$$\dot{\tilde{K}}_e = -\frac{1}{\alpha} x_e \tilde{F}_s \quad (82)$$

where  $\alpha$  is a positive scalar. Equation (82) can be rearranged to give the following adaptation rule, which can directly be implemented on the system.

$$\hat{K}_e = K_o + \int (\alpha x_e^2 \hat{K}_e - \alpha x_e F) \quad (83)$$

It should be noted here that, existence of the persistent excitation condition is assumed to be satisfied. Moreover, in order to have a fast update, the adaptation coefficient  $\alpha$  should be picked relatively high. A depiction of the overall structure including the position control and force controller with parameter adaptation is given in Figure 3.12 below.

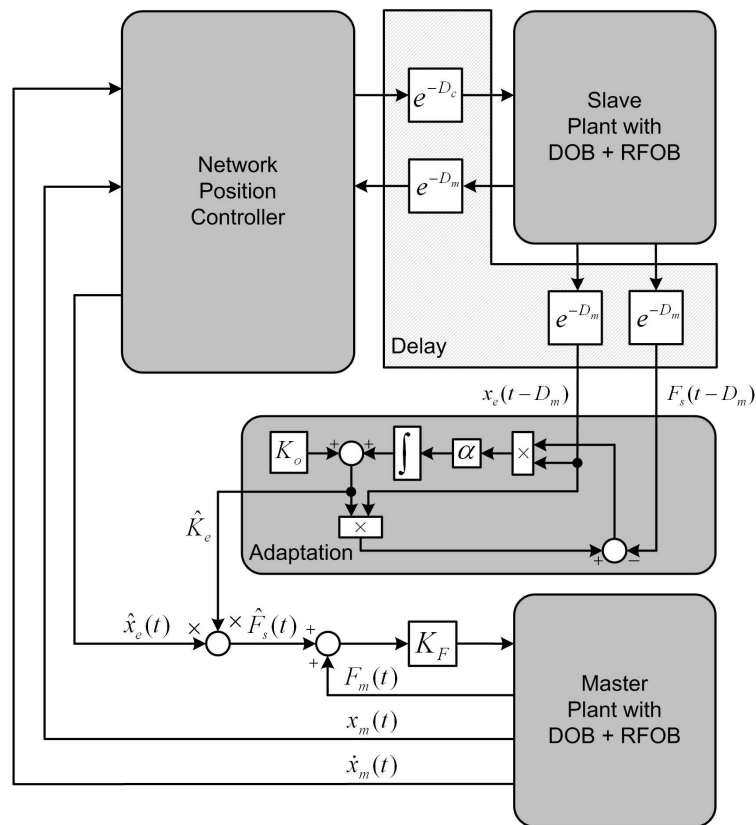


Figure 3.12: Block diagram of the overall controller

### 3.2.3 Experimental Results

The proposed adaptation scheme is tested on the experiments. The results obtained from this controller structure is shown in Figure 3.13 below. During the experiment, the initial conditions for the environment stiffness was

selected as  $K_e = 10N/m$ . Looking at the results, it is clear that for the first contact with environment, the controller cannot recover the slave force. But during first interaction it can estimate the stiffness and before the second contact with environment, master side can have a prediction of the slave force. Actual slave force follows after the delay. Moreover, due to the continuous estimation, as more interaction with environment is made, the estimated value approximates to the actual value more and thus force tracking error between the estimated and actual slave force decreases.

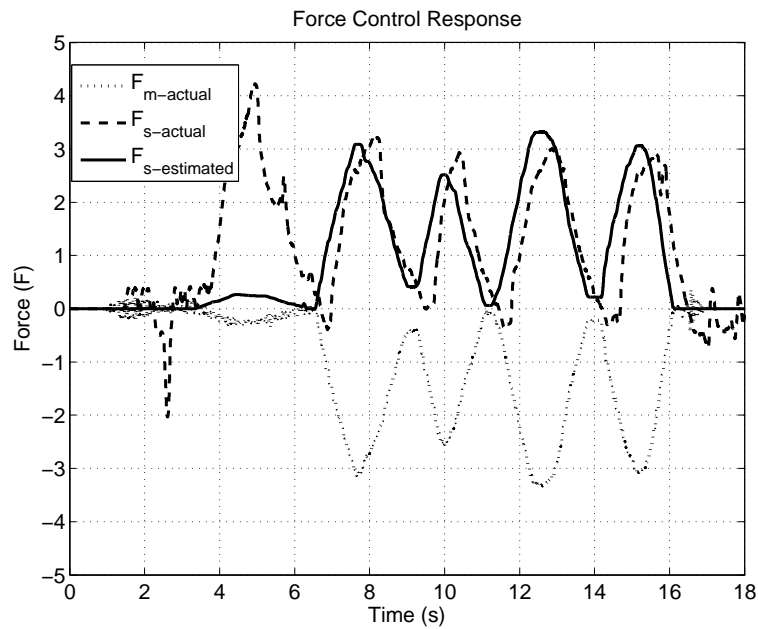


Figure 3.13: Adaptive force reconstruction experiment

# Chapter IV

## 4 Conclusion & Future Works

In this thesis bilateral control is analyzed and experimentally evaluated on a master-slave teleoperation system. The obtained results show the possibility of using DOB and acceleration control framework for bilateral control. Disturbance observer enables combining position control and force control in the acceleration dimension so that two control objectives can naturally be coupled.

Using a similar functional relationship between master and slave systems, it is shown that grasping control can be formulated and solved with the same DOB based idea. Under the assumption that the controller has apriori knowledge of object parameters, a novel control structure is developed in which both force and position could track their references. In comparison to the bilateral control of a remote object, in grasping control the availability of known force reference enabled the use of the derivative of force reference which improved the overall controller performance. Adopting from this observation, it can be noted that the performance of general bilateral control can be improved if very accurate observation of the derivative of force is available to the controller.

In the last part of chapter II, performance improvement with better ob-

servers is discussed. In that context, a new functional observer is proposed and experimentally validated. The results indicate that making use of input current in the observer can enhance the estimation performance resulting in faster response. This way, it is possible to use double filter in the observer and obtain smoother responses that is fast enough to satisfy the desired bandwidth.

In chapter III, bilateral teleoperation with time delay is analyzed. Splitting the general problem into two parts, position and force control of a time delayed bilateral control system are investigated differently.

First, position control of a time delayed bilateral system is analyzed. It is verified that the structure proposed in [42] can be used for position control under time delay. Tracking performance of this scheme is quite satisfactory even under large uncertain delay ranges. Observation is made about the deficient tracking performance of slave system when there is contact with environment. This problem is solved with a model following control that makes use of a virtual slave plant without environment. Utilizing a discrete time sliding mode controller it is shown that position tracking of master system reference by the slave system is satisfied even though there is interaction with environment.

Other than the position control, force control under time delay is also investigated in the last section of chapter III. For force control, first a local controller is implemented that makes use of the delayed force from the slave plant. Although this controller could provide stable operation, it was way beyond transparent operation due to the delayed force feedback. In order catch a better transparency for force control, a new structure is proposed. In this new structure, an adaptation scheme is used to estimate the environment



stiffness. Under the assumption that environment location is known by the master system, estimated environment parameters are used to close the force loop on the master side. This way, the operator could feel the slave forces before they actually exist and the operation transparency is improved.

For further study, the adaptation algorithm is planned to be extended. First integration of this adaptive scheme with the position controller should be made in a unique structure, so that the resulting system can keep two coupled loops instead of two separate loops. Moreover, changing the environment model to a nonlinear spring damper system would result in a better force estimation for viscous and hard contact environments.

As a part of future work, it is also planned try new predictive structures to compensate (partially if not fully) the delay in the input channel. This way the overall effect of time delay can be reduced and the closed loop system performance can be improved even further.

## References

- [1] N. Hogan, "Impedance Control: An approach to manipulation: Parts I-III.", *ASME Journal of Dynamic Systems, Measurement and Control*, vol. 107, no. 1, pp. 1-24, Mar. 1985
- [2] J. E. Colgate, "Robust Impedance Shaping Telemanipulation", *IEEE Transactions on Robotics and Automation*, vol. 9, no. 4, pp. 374-384, Aug. 1993
- [3] D. A. Lawrence, "Stability and Transparency in Bilateral Teleoperation", *Proceedings of the 31st Conference on Decision and Control*, Tuscon-Arizona, USA, Dec. 1992, pp 2649-2655
- [4] E. W. Kamen, P. P. Khargonekar and A. Tanenbaum, "Stabilization of time-delay systems using finite dimensional compensators", *IEEE Transactions on Automatic Control*, vol. 30, No. 1, pp. 75-78, Jan. 1985
- [5] A. Kojima and S. Ishjiama "Robust controller design for delay systems in the Gap-Metric", *IEEE Transactions on Automatic Control*, vol. 40, No. 2, pp. 370-374, Feb. 1995
- [6] S. U. Niculescu, M. Fu and H. Li, "Delay dependent closed loop stability of linear systems with input delay: An LMI approach", *Proceedings of the 36st Conference on Decision and Control*, San Diego, USA, Dec. 1997, pp 1623-1628
- [7] S. Khan, A. Sabanovic and A. O. Nergiz, "Scaled Bilateral Teleoperation Using Discrete-Time Sliding-Mode Controller", *IEEE Transactions on Industrial Electronics*, vol. 56, No. 9, pp. 3609-3618, Sep. 2009

- [8] N. Ando, P. Korondi and H. Hashimoto, "Development of Micro-manipulator and Haptic Interface for Networked Micromanipulation", *IEEE/ASME Transactions on Mechatronics*, vol. 6, No. 4, pp. 417-427, Dec. 2001
- [9] E. V. Poorten, T. Kanno and Y. Yokokohji, "Robust Variable-Scale Bilateral Control for Micro Teleoperation", *IEEE International Conference on Robotics and Automation (ICRA)*, Pasadena, CA, USA, May 2008, pp 655-662
- [10] C. D. Onal and M. Sitti, "A Scaled Bilateral Control System for Experimental One-dimensional Teleoperated Nanomanipulation", *The International Journal of Robotics Research*, vol. 28, No. 4, pp. 484-497, 2009
- [11] C. D. Onal and M. Sitti, "Teleoperated 3-D Force Feedback From the Nanoscale With an Atomic Force Microscope", *IEEE Transactions on Nanotechnology*, vol. 9, No. 1, pp. 46-54, Jan. 2010
- [12] S. Katsura, T. Suzuyama and K. Ohnishi, "A Realization of Multilateral Force Feedback Control for Cooperative Motion", *IEEE Transactions on Industrial Electronics*, vol. 54, No. 6, pp. 3298-3306, Dec. 2007
- [13] S. Katsura, Y. Matsumoto and K. Ohnishi, "Realization of "Law of Action and Reaction" by Multilateral Control", *IEEE Transactions on Industrial Electronics*, vol. 52, No. 5, pp. 1196-1205, Oct. 2005
- [14] S. Katsura and K. Ohnishi, "A Realization of Haptic Training System by Multilateral Control", *IEEE Transactions on Industrial Electronics*, vol. 53, No. 6, pp. 1935-1942, Dec. 2006

- [15] R. Kubo, T. Shimono and K. Ohnishi, "Flexible Controller Design of Bilateral Grasping Systems Based on a Multilateral Control Scheme", *IEEE Transactions on Industrial Electronics*, vol. 56, No. 1, pp. 62-68, Jan. 2009
- [16] R. C. Goertz, "Mechanical Master-Slave Manipulator", *Nucleonics*, vol. 12, no. 11, pp 45-46, May 1954.
- [17] W. R. Ferrel, "Remote Manipulation with Transmission Delay", *IEEE Transactions on Human Factors in Electronics*, vol. 6, pp 24-32, 1965.
- [18] W. R. Ferrel and T. B. Sheridan, "Supervisory Control of Remote Manipulation", *IEEE Spectrum*, pp 81-88, 1967.
- [19] F. Miyazaki, S. Matsubayashi, T. Yoshimi, S. Arimoto, "A New Control Methodology Toward Advanced Teleoperation of Master-Slave Robot Systems", *IEEE International Conference on Robotics and Automation (ICRA)*, May 1989, pp 997-1002
- [20] B. Hannaford and P. Fiorini, "A Detailed Model of Bi-Lateral Teleoperation", *IEEE International Conference on Systems Man and Cybernetics*, 1988, pp 117-121
- [21] G. J. Raju, G. C. Verghese, T. B. Sheridan, "Design Issues in 2-Port Network Models of Bilateral Remote Manipulation", *IEEE International Conference on Robotics and Automation (ICRA)*, May 1989, pp 1316-1321
- [22] R. J. Anderson and M. W. Spong, "Bilateral Control of Teleoperators with Time Delay", *IEEE Transactions on Automatic Control*, vol. 34, no. 5, pp 494-501, May 1989.

- [23] G. Niemeyer and J. Slotine, "Stable Adaptive Teleoperation", *IEEE Journal of Ocean Engineering*, vol. 16, no. 1, pp 152-162, Jan. 1991.
- [24] G. Niemeyer, "Using Wave Variables in the Time Delayed Force Reflecting Teleoperation", *PhD Thesis, MIT, Cambridge, MA*, 1996.
- [25] G. Niemeyer and J. J. E. Slotine, "Towards Force-Reflecting Teleoperation Over the Internet", *IEEE International Conference on Robotics and Automation (ICRA)*, Leuven, Belgium, May 1998, pp 1909-1915
- [26] K. Kawashima, K. Tadano, G. Sankaranarayanan, B. Hannaford, "Bilateral Teleoperation with Time Delay using Modified Wave Variables", *IEEE International Conference on Intelligent Robots and Systems (IROS)*, Nice, France, September 2008, pp 424-429
- [27] Y. Yokokohji, T. Imaida, T. Yoshikawa, "Bilateral Teleoperation under Time Varying Communication Delay", *IEEE/RJS International Conference on Intelligent Robots and Systems (IROS)*, Kyongju, South Korea, Oct. 1999, pp 1854-1859
- [28] S. Munir and W. J. Book, "Internet Based Teleoperation using Wave Variables with Prediction", *IEEE/ASME International Conference on Intelligent Mechatronics*, Como, Italy, July 2001, pp 43-50
- [29] G. Niemeyer and J. J. E. Slotine, "Telemanipulation with Time Delays", *International Journal of Robotics Research*, vol. 23, no. 9, pp 873-890, Sep. 2004.
- [30] J. H. Ryu, D. S. Kwon, B. Hannaford, "Stable Teleoperation with Time Domain Passivity Control", *IEEE Transactions on Robotics and Automation*, vol. 20, no. 2, pp 365-373, April 2004.

- [31] J. H. Ryu, C. Preusche, "Stable Bilateral Control of Teleoperators Under Time-Varying Communication Delay: Time Domain Passivity Approach", *IEEE International Conference on Robotics and Automation (ICRA)*, Rome, Italy, April 2007, pp 3508-3513
- [32] N. Chopra, M. W. Spong, R. Ortega, N. E. Barabanov, "On Tracking Performance in Bilateral Teleoperation", *IEEE Transactions on Robotics*, vol. 22, no. 4, pp 861-866, August 2006.
- [33] K. Hashtrudi-Zaad and S. E. Salcudean, "Transparency in Time Delayed Systems and the Effects of Local Force Feedback for Transparent Teleoperation", *IEEE Transactions on Robotics and Automation*, vol. 18, no. 1, pp 108-114, February 2002.
- [34] V. Massimiliano, "Performance Improvement of Smith Predictor Through Automatic Computation of Dead Time", *Technical Report*, April 2003, pp 25-30
- [35] K. Hashtrudi-Zaad and S. E. Salcudean, "Adaptive Transparent Impedance Reflecting Teleoperation", *IEEE International Conference on Robotics and Automation (ICRA)*, April 1996, pp 1369-1374
- [36] J. E. Colgate, "Robust Impedance Shaping Telemanipulation", *IEEE Transactions on Robotics and Automation*, vol. 9, no. 4, pp 374-384, August 1993.
- [37] T. Slama, D. Aubry, R. Oboe, F. Kratz, "Robust Bilateral Generalized Predictive Control for Teleoperation Systems", *Mediterranean Conference on Control and Automation*, June 2007, pp 1-6

- [38] G. M. H. Leung, B. A. Francis, J. Apkarian, "Bilateral Controller for Teleoperators with Time Delay via  $\mu$ -Synthesis", *IEEE Transactions on Robotics and Automation*, vol. 11, no. 1, pp 105-116, 1995.
- [39] K. Natori, "Time Delay Compensation for Motion Control Systems", *PhD Thesis, Keio University, Yokohama, Japan*, 2008.
- [40] K. Natori, R. Oboe, K. Ohnishi, "Analysis and Design of Time Delayed Control Systems with Communication Disturbance Observer", *IEEE International Symposium on Industrial Electronics*, Vigo, Spain, June 2007, pp 3132-3137
- [41] K. Natori, T. Tsuji, K. Ohnishi, "Time Delay Compensation by Communication Disturbance Observer in Bilateral Teleoperation Systems", *IEEE International Workshop on Advanced Motion Control*, Istanbul, Turkey, March 2006, pp 218-223
- [42] A. Sabanovic, K. Ohnishi, D. Yashiro, M. Acer, N. S. Behlilovic, "Control Systems with Network Delay", *International Conference on Electrical Drives and Power Electronics*, Dubrovnik, Croatia, October 2009
- [43] A. Sabanovic, K. Ohnishi, D. Yashiro, N. Sabanovic, "Motion Control Systems with Network Delay", *The 35th Annual Conference of IEEE Industrial Electronics Society (IECON)*, Porto, Portugal, November 2009, pp 2297-2302
- [44] K. Kawashima, K. Tadano, G. Sankaranarayanan, B. Hannaford, "Model-Based Passivity Control for Bilateral Teleoperation of a Surgical Robot with Time Delay", *IEEE International Conference on In-*

*telligent Robots and Systems (IROS)*, Nice, France, September 2008, pp 1427-1432

- [45] K. Kitamura, D. Yashiro, K. Ohnishi, "Bilateral Control Using Estimated Environmental Stiffness as the Master Position Gain", *The 35th Annual Conference of IEEE Industrial Electronics Society (IECON)*, Porto, Portugal, November 2009, pp 2981-2986
- [46] E. J. R. Seda, D. Lee, M. W. Spong, "An Experimental Comparison Study for Bilateral Internet-Based Teleoperation", *IEEE International Conference on Control Applications*, Munich, Germany, Oct. 2006, pp 1701-1706
- [47] G. Sankaranarayanan and B. Hannaford, "Experimental Comparison of Internet Haptic Collaboration with Time-Delay Compensation Techniques", *IEEE International Conference on Robotics and Automation (ICRA)*, Pasadena, CA, USA, May 2008, pp 206-211
- [48] P. F. Hokayem and M. W. Spong, "Bilateral teleoperation: An historical survey", *Automatica*, vol. 42, no. 12, pp 2035-2057, September 2006.
- [49] T. B. Sheridan, "Space Teleoperation Through Time Delay: Review and Prognosis", *IEEE Transactions on Robotics and Automation*, vol. 9, no. 5, pp. 592-606, Oct. 1993.
- [50] Y. Matsumoto, S. Katsura and K. Ohnishi "An Analysis and Design of Bilateral Control Based on Disturbance Observer", *IEEE International Conference on Information Technology (ICIT)*, Maribor, Slovenia, May 2004, pp 802-807



- [51] E. Ishii, S. Katsura, H. Nishi, K. Ohnishi, "Bilateral Teleoperation Based on Modal System Design", *IEEE International Symposium on Industrial Electronics (ISIE)*, Dubrovnik, Croatia, June 2005, pp 1527-1532
- [52] A. Sabanovic, K. Ohnishi, "Fundamentals of Motion Control Systems", *Yet not published*
- [53] R. L. Hollis, S. Salcudean, and D. W. Abraham, "Toward a tele-nanorobotic manipulation system with atomic scale force feedback and motion resolution", *Proceedings of MEMS*, pp. 115-119, 1990.
- [54] K. Chin, "Stable teleoperation with scaled feedback", *MIT, Laboratory for Information and Decision Systems*, pp. 1-13, 1993.
- [55] S. E. Salcudean, S. Ku and G. Bell, "Performance Measurement in Scaled Teleoperation for Microsurgery", *Lecture Notes in Computer Science*, vol. 12, no. 5, pp 789-798, April 2006.
- [56] M. Boukhnifer and A. Ferreira, "Stability and Transparency for Scaled Teleoperation System", *IEEE International Conference on Robotics and Automation (ICRA)*, Beijing, China, Oct 2006, pp 4217-4222
- [57] G. Li, N. Xi, M. Yu and W. K. Fung, "Development of Augmented Reality System for AFM-Based Nanomanipulation", *IEEE/ASME Transactions on Mechatronics*, vol. 9, no. 2, pp. 358-365, June, 2004.
- [58] C. D. Onal and M. Sitti, "A Scaled Bilateral Control System for Experimental One-dimensional Teleoperated Nanomanipulation", *The International Journal of Robotics Research*, vol. 28, no. 4, pp. 484-497, April 2009.

- [59] R. Kubo, T. Shimono and K. Ohnishi, "Flexible Controller Design of Bilateral Grasping Systems Based on a Multilateral Control Scheme", *IEEE Transactions on Industrial Electronics*, vol. 56, no. 1, pp. 62-68, Jan. 2009.
- [60] S. Katsura and K. Ohnishi, "A Realization of Haptic Training System by Multilateral Control", *IEEE Transactions on Industrial Electronics*, vol. 53, no. 6, pp. 1935-1942, Dec. 2006.
- [61] S. Katsura, T. Suzuyama and K. Ohishi, "A Realization of Multilateral Force Feedback Control for Cooperative Motion", *IEEE Transactions on Industrial Electronics*, vol. 54, no. 6, pp. 3298-3306, Dec. 2007.
- [62] S. Katsura and K. Ohishi, "Modal System Design of Multirobot Systems by Interaction Mode Control", *IEEE Transactions on Industrial Electronics*, vol. 54, no. 3, pp. 1537-1546, June. 2007.
- [63] S. Sirouspour and P. Setoodeh, "Multi-operator/Multi-robot Teleoperation: An Adaptive Nonlinear Control Approach", *IEEE International Conference on Intelligent Robots and Systems (IROS)*, Alberta, Canada, August 2005, pp. 1576-1581
- [64] G. Hwang, H. Hashimoto, P. Szemans and N. Ando, "An Evaluation of Grasp Force Control in Single-Master Multi-Slave Tele-Micromanipulation", *IEEE International Conference on Intelligent Robots and Systems (IROS)*, Alberta, Canada, August 2005, pp 2179-2184

- [65] S. Sirouspour, "Modeling and Control of Cooperative Teleoperation Systems", *IEEE Transactions on Robotics*, vol. 21, no. 6, pp. 1220-1225, Dec. 2005.
- [66] K. Ogata, "System Dynamics", *Prentice Hall*, 2003
- [67] K. Ohnishi, M. Shibata, T. Murakami, "Motion Control for Advanced Mechatronics", *IEEE Transactions on Mechatronics*, vol. 1, no. 1, pp 56-67, 1996.
- [68] T. Murakami, F. Yu, K. Ohnishi, "Torque Sensorless Control in Multidegree-of-Freedom Manipulator", *IEEE Transactions on Industrial Electronics*, vol. 40, no. 2, pp 259-265, 1993.
- [69] J. P. Richard "Time-delay systems: and overview of some recent advances and open problems", *Automatica*, vol. 39, no. 10, pp 1667-1694, 2003.
- [70] C. Onal, "Bilateral Control: A Sliding Mode Approach", *PhD Thesis*, *Sabanci University, Istanbul, Turkey*, 2005.

## VITA

Abdurrahman Eray Baran  
Candidate for the Degree of  
Master of Science

Thesis: Disturbance Observer Based Bilateral Control Systems

Major Field: Mechatronics Engineering

Biographical:

Abdurrahman Eray Baran was born in Diyarbakir, Turkey. He received his B.S. degree in Mechatronics Engineering from Sabanci University, Istanbul, Turkey in 2008. His research interests include motion control systems, time delayed systems, bilateral control systems, estimation and observers.

The following were published out of this thesis:

- A. Sabanovic, K. Ohnishi, D. Yashiro, N. Sabanovic, E. A. Baran, "Motion Control Systems with Network Delay", *Automatika*, vol. 51, no. 2, pp 119-126, June 2010 (SCI)
- E. A. Baran, E. Golubivic, A. Sabanovic, "A new Functional Observer to Estimate Velocity, Acceleration and Disturbance for Motion Control Systems" (In Proceedings of the IEEE International Symposium on Industrial Electronics - ISIE 2010)
- E. A. Baran, A. Sabanovic, "A Robust Grasping Force Controller" In Proceedings of the Turkish Automatic Control Conference, Istanbul, TURKEY, October 2009